


Non-Fermi liquid fixed point of the dissipative Yukawa-Sachdev-Ye-Kitaev model

Niklas Cichutek , Andreas Rückriegel, Max O. Hansen, and Peter Kopietz

Institut für Theoretische Physik, Universität Frankfurt, Max-von-Laue Straße 1, 60438 Frankfurt, Germany



(Received 1 January 2024; accepted 18 March 2024; published 1 April 2024)

Using a functional renormalization group approach we derive the renormalization group (RG) flow of a dissipative variant of the Yukawa-Sachdev-Ye-Kitaev model describing N fermions on a quantum dot, which interact via a disorder-induced Yukawa coupling with M bosons. The inverse Euclidean propagator of the bosons is assumed to exhibit a nonanalytic term proportional to the modulus of the Matsubara frequency. We show that, to leading order in $1/N$ and $1/M$, the hierarchy of formally exact flow equations for the irreducible vertices of the disorder-averaged model can be closed at the level of the two-point vertices. We find that the RG flow exhibits a non-Fermi liquid fixed point characterized by a finite fermionic anomalous dimension η , which is related to the bosonic anomalous dimension γ via the scaling law $2 = 2\eta + \gamma$ with $0 < \eta < 1/2$. We explicitly calculate η and the critical exponents characterizing the linearized RG flow in the vicinity of the fixed point as functions of N/M .

DOI: [10.1103/PhysRevB.109.155101](https://doi.org/10.1103/PhysRevB.109.155101)

I. INTRODUCTION

The Yukawa-Sachdev-Ye-Kitaev (YSYK) model describes N fermions on a quantum dot, which are coupled to M phonons via infinite-range random couplings [1–9]. Recently this model has also attracted attention because it features maximally chaotic behavior [7,10]. In the limit $N \rightarrow \infty$ and $M \rightarrow \infty$ with $N/M = \mathcal{O}(1)$ (which we call for simplicity large- N limit) the YSYK model exhibits a non-Fermi liquid state, which can be studied in a controlled way. In this limit the perturbative expansion of the fermionic and bosonic self-energies is dominated by so-called melon diagrams, which can be summed to all orders in perturbation theory by solving coupled Dyson-Schwinger (DS) equations. Alternatively, the DS equations can be derived from the large- N saddle point of a suitably defined functional integral involving special bilocal composite fields [1,11,12]. From the numerical solution of the DS equations for the YSYK model Pan *et al.* [5] have shown that the model exhibits for vanishing chemical potential μ a non-Fermi liquid phase where the fermionic and bosonic self-energies display power-law behavior characterized by exponents, which depend on the ratio N/M . Moreover, the power-law behavior of the self-energies persists even for finite values of μ , a phenomenon, which has been called *self-tuned* criticality [5]. The leading power-law behavior in the non-Fermi liquid phase has also been extracted analytically by self-consistently solving the DS equation at low energies [6]. However, the physical reason for the self-tuned criticality of the non-Fermi liquid phase of the YSYK model has not been identified.

From the point of view of the renormalization group (RG) the phenomenon of self-tuned criticality has a simple explanation: the critical state must be associated with a fixed point with only attractive directions. Such a fixed point is called a sink [13–15] and describes a stable phase of matter. In fact, the non-Fermi liquid phase of the Sachdev-Ye-Kitaev model with complex fermions has recently been shown to be associated with such a sink [15]. Unfortunately, we have not

been able to obtain sensible results for the critical behavior of the YSYK model using a straightforward generalization of the functional renormalization group (FRG) approach developed in our previous paper [15] for the SYK model. The reason for this failure of the standard FRG approach are not entirely clear to us at this point; possible explanations are the failure of the low-energy expansion or subtleties associated with the proper regulator choice in coupled Fermi-Bose systems with two types of frequency scaling [16]. It turns out, however, that these technical complications do not arise for the dissipative variant of the YSYK model where the frequency dependence of the inverse boson propagator is proportional to the modulus $|\Omega|$ of the bosonic Matsubara frequency. In this paper we will therefore focus on this dissipative YSYK model and use a generalization of the FRG approach developed in Ref. [15] to investigate the RG flow of this model. Our motivation for studying this model is not solely technical, because the dissipative YSYK model can be viewed as a toy model for understanding the behavior of strongly correlated fermions that are coupled to bosons with dissipative dynamics.

We define the dissipative YSYK model via the following Euclidean action,

$$S = S_2 + \frac{1}{\sqrt{MN}} \sum_{ijk} g_{ijk} \sum_{\sigma} \int_0^{\beta} d\tau \bar{c}_{i\sigma}(\tau) c_{j\sigma}(\tau) \phi_k(\tau), \quad (1.1)$$

where β is the inverse temperature, $\phi_k(\tau)$ is a real bosonic field depending on a flavor index k and imaginary time τ , $c_{i\sigma}(\tau)$ and $\bar{c}_{i\sigma}(\tau)$ are Grassmann variables representing electrons of type i with spin projection σ , and the quadratic part of the action is in frequency space given by

$$S_2 = -\frac{1}{\beta} \sum_{\omega} \sum_{i=1}^N \sum_{\sigma} (i\omega + \mu) \bar{c}_{i\sigma\omega} c_{i\sigma\omega} + \frac{1}{2\beta} \sum_{\Omega} \sum_{k=1}^M (|\Omega| + \Delta) \phi_{k\Omega}^* \phi_{k\Omega}. \quad (1.2)$$

Here Δ defines the bare energy scale of the bosons, ω and Ω are fermionic and bosonic Matsubara frequencies, and the Fourier components of the fields are defined by

$$c_{i\sigma\omega} = \int_0^\beta d\tau e^{i\omega\tau} c_{i\sigma}(\tau), \quad \phi_{k\Omega} = \int_0^\beta d\tau e^{i\Omega\tau} \phi_k(\tau). \quad (1.3)$$

The Yukawa couplings g_{ijk} in Eq. (1.1) are independent Gaussian random variables with vanishing average and constant variance. In general the couplings $g_{ijk} = g'_{ijk} + ig''_{ijk}$ are complex. The Hermiticity of the Hamiltonian implies that the real and imaginary parts have the symmetries $g'_{ijk} = g'_{jik}$ and $g''_{ijk} = -g''_{jik}$. A finite imaginary part g''_{ijk} is a manifestation of broken time-reversal symmetry [6]. The second moments of the couplings are assumed to be of the form [6]

$$\langle g'_{ijk} g'_{i'j'k'} \rangle = g_1^2 (\delta_{ii'} \delta_{jj'} + \delta_{ij'} \delta_{j'i'}) \delta_{kk'}, \quad (1.4a)$$

$$\langle g''_{ijk} g''_{i'j'k'} \rangle = g_2^2 (\delta_{ii'} \delta_{jj'} - \delta_{ij'} \delta_{j'i'}) \delta_{kk'}, \quad (1.4b)$$

$$\langle g'_{ijk} g''_{i'j'k'} \rangle = 0, \quad (1.4c)$$

where $\langle \dots \rangle$ denotes averaging over the Gaussian probability distribution of the random couplings. The nonanalytic $|\Omega|$ dependence in the bosonic part of S_2 describes dissipative bosonic dynamics due to the coupling to some other degrees of freedom that do not explicitly appear in the above action. Note that the usual YSYK model can be obtained by replacing $|\Omega| \rightarrow \Omega^2$ in Eq. (1.2).

The rest of this paper is organized as follows. In Sec. II we derive FRG flow equations for the irreducible vertices of the disorder-averaged YSYK model and develop a truncation of the hierarchy of FRG flow equations, which becomes exact for $N \rightarrow \infty$ and $M \rightarrow \infty$. The resulting flow equations are not precisely equivalent to the DS equations [1–9] for the YSYK model. However, the DS equations can be recovered if we modify our flow equations using the so-called Katanin substitution [17]. In Sec. III we simplify our FRG flow equations for the irreducible self-energies using a standard low-energy expansion, which reduces our functional flow equations to a system of ordinary differential equations for five scale-dependent couplings associated with the chemical potential, the boson gap, and three types of wave-function renormalization factors. In Sec. IV we show that our flow equations have a nontrivial non-Fermi liquid fixed point. We

derive the linearized RG flow in the vicinity of this fixed point and show that it has only one repulsive direction corresponding to a linear combination of the rescaled chemical potential and a parameter describing the spectral asymmetry. All other couplings are irrelevant at this fixed point, so that fine-tuning of the bosonic energy scale Δ in Eq. (1.2) is not necessary to realize the non-Fermi liquid phase. Finally, in Sec. V we present our conclusions.

II. LARGE- N TRUNCATION OF THE EXACT RG FLOW EQUATIONS

To calculate the disorder average of the grand canonical potential and of the correlation functions of our model we should use the replica trick [1]. Note that for the SYK model with Majorana fermions replica-nonsymmetric large- N saddle points with energies lower than the replica-symmetric saddle point have been found [18]. Whether this happens also for the YSYK model has not been thoroughly investigated. Here we assume that the replica symmetry is not broken, so that we can simply average the partition function and treat the g_{ijk} as additional complex fields, which should be integrated over. The average partition function can be written as

$$\langle \mathcal{Z} \rangle = \int \mathcal{D}[c, \bar{c}, \phi] e^{-S_2} \times \langle e^{-\frac{1}{\sqrt{NM}} \sum_{ijk} g_{ijk} \sum_{\sigma} \int_0^\beta d\tau \bar{c}_{i\sigma}(\tau) c_{j\sigma}(\tau) \phi_k(\tau)} \rangle. \quad (2.1)$$

Since the probability distribution of the g_{ijk} is Gaussian, the averaging in Eq. (2.1) generates the usual Debye-Waller factor,

$$\langle \mathcal{Z} \rangle = \int \mathcal{D}[c, \bar{c}, \phi] e^{-S_2 - S_6}, \quad (2.2)$$

where the interaction S_6 involves six powers of the fields,

$$S_6 = -\frac{1}{2NM} \sum_{ijk} \sum_{i'j'k'} \langle g_{ijk} g_{i'j'k'} \rangle \sum_{\sigma\sigma'} \int_0^\beta d\tau \int_0^\beta d\tau' \times \bar{c}_{i\sigma}(\tau) c_{j\sigma}(\tau) \phi_k(\tau) \bar{c}_{i'\sigma'}(\tau') c_{j'\sigma'}(\tau') \phi_{k'}(\tau'). \quad (2.3)$$

Using our assumptions (1.4) for the second moments we obtain

$$\begin{aligned} S_6 &= -\frac{1}{2MN} \sum_{ijk} \sum_{\sigma\sigma'} \int_0^\beta d\tau \bar{c}_{i\sigma}(\tau) c_{j\sigma}(\tau) \phi_k(\tau) \int_0^\beta d\tau' \{ g_1^2 [\bar{c}_{i\sigma'}(\tau') c_{j\sigma'}(\tau') + (i \leftrightarrow j)] - g_2^2 [\bar{c}_{i\sigma'}(\tau') c_{j\sigma'}(\tau') - (i \leftrightarrow j)] \} \phi_k(\tau') \\ &= -\frac{1}{2MN} \sum_{ijk} \sum_{\sigma\sigma'} \int_0^\beta d\tau \int_0^\beta d\tau' \phi_k(\tau) \phi_k(\tau') \{ (g_1^2 - g_2^2) \bar{c}_{i\sigma}(\tau) c_{j\sigma}(\tau) \bar{c}_{i\sigma'}(\tau') c_{j\sigma'}(\tau') \\ &\quad + (g_1^2 + g_2^2) \bar{c}_{i\sigma}(\tau) c_{j\sigma}(\tau) \bar{c}_{j\sigma'}(\tau') c_{i\sigma'}(\tau') \} \\ &= -\frac{1}{4MN} \sum_{ijk} \sum_{\sigma\sigma'} \int_0^\beta d\tau \int_0^\beta d\tau' \phi_k(\tau) \phi_k(\tau') \{ g_1^2 [\bar{c}_{i\sigma}(\tau) c_{j\sigma}(\tau) + (i \leftrightarrow j)] [\bar{c}_{i\sigma'}(\tau') c_{j\sigma'}(\tau') + (i \leftrightarrow j)] \\ &\quad - g_2^2 [\bar{c}_{i\sigma}(\tau) c_{j\sigma}(\tau) - (i \leftrightarrow j)] [\bar{c}_{i\sigma'}(\tau') c_{j\sigma'}(\tau') - (i \leftrightarrow j)] \}. \end{aligned} \quad (2.4)$$

In frequency space this interaction can be written as

$$S_6 = -\frac{1}{2NM\beta^6} \sum_{n'_1, n'_2, n_2, n_1} \sum_{\sigma'_1, \sigma'_2, \sigma_2, \sigma_1} \sum_{\omega'_1, \omega'_2, \omega_2, \omega_1} \sum_{k_1, k_2} \sum_{\Omega_1, \Omega_2} \beta \delta_{\omega'_1 + \omega'_2, \omega_2 + \omega_1 + \Omega_2 + \Omega_1} \beta \delta_{\omega'_2, \omega_2 + \Omega_2} \delta_{k_1, k_2} \\ \times \left\{ (g_1^2 - g_2^2) \delta_{\sigma'_1, \sigma_1} \delta_{\sigma'_2, \sigma_2} \delta_{n'_1, n'_2} \delta_{n_1, n_2} + (g_1^2 + g_2^2) \delta_{\sigma'_1, \sigma_1} \delta_{\sigma'_2, \sigma_2} \delta_{n'_1, n_2} \delta_{n'_2, n_1} \right\} \bar{c}_{1'} \bar{c}_{2'} c_2 c_1 \phi_{k_1 \Omega_1} \phi_{k_2 \Omega_2}, \quad (2.5)$$

where we have introduced the abbreviations $1 = (n_1, \sigma_1, \omega_1)$, $1' = (n'_1, \sigma'_1, \omega'_1)$ etc. for the fermionic labels. A graphical representation of the nonsymmetrized interaction vertices in Eq. (2.6) is shown in Fig. 1. For the derivation of formally exact FRG flow equations it is convenient to work with vertices, which are antisymmetric with respect to permutation of the outgoing and the incoming fermion labels, and symmetric with respect to permutation of the boson labels. Therefore we write the bare interaction S_6 in the symmetrized form

$$S_6 = \frac{1}{(2!)^3 NM \beta^6} \sum_{n'_1, n'_2, n_2, n_1} \sum_{\sigma'_1, \sigma'_2, \sigma_2, \sigma_1} \sum_{\omega'_1, \omega'_2, \omega_2, \omega_1} \sum_{k_1, k_2} \sum_{\Omega_1, \Omega_2} \beta \delta_{\omega'_1 + \omega'_2, \omega_2 + \omega_1 + \Omega_2} \Gamma_0^{\bar{c}\bar{c}cc\phi\phi}(1', 2'; 2, 1; k_1 \Omega_1, k_2 \Omega_2) \bar{c}_{1'} \bar{c}_{2'} c_2 c_1 \phi_{k_1 \Omega_1} \phi_{k_2 \Omega_2}, \quad (2.6)$$

where the mixed six-point vertex $\Gamma_0^{\bar{c}\bar{c}cc\phi\phi}(1', 2'; 2, 1; k_1 \Omega_1, k_2 \Omega_2)$ is antisymmetric with respect to the exchange $1' \leftrightarrow 2'$ and $1 \leftrightarrow 2$, and symmetric with respect to the exchange $k_1 \Omega_1 \leftrightarrow k_2 \Omega_2$. Explicitly, the bare value of the properly symmetrized mixed six-point vertex is

$$\Gamma_0^{\bar{c}\bar{c}cc\phi\phi}(n'_1 \sigma'_1 \omega'_1, n'_2 \sigma'_2 \omega'_2; n_2 \sigma_2 \omega_2, n_1 \sigma_1 \omega_1; k_1 \Omega_1, k_2 \Omega_2) \\ = -\delta_{k_1 k_2} \frac{\beta}{2} \left\{ (g_1^2 + g_2^2) [\delta_{n'_1 n_2} \delta_{n'_2 n_1} \delta_{\sigma'_1 \sigma_1} \delta_{\sigma'_2 \sigma_2} (\delta_{\omega'_1, \omega_1 + \Omega_1} + \delta_{\omega'_2, \omega_2 + \Omega_2}) - \delta_{n'_2 n_2} \delta_{n'_1 n_1} \delta_{\sigma'_2 \sigma_1} \delta_{\sigma'_1 \sigma_2} (\delta_{\omega'_2, \omega_1 + \Omega_1} + \delta_{\omega'_1, \omega_2 + \Omega_2})] \right. \\ \left. + (g_1^2 - g_2^2) \delta_{n'_1 n'_2} \delta_{n_1 n_2} [\delta_{\sigma'_1 \sigma_1} \delta_{\sigma'_2 \sigma_2} (\delta_{\omega'_1, \omega_1 + \Omega_1} + \delta_{\omega'_2, \omega_2 + \Omega_2}) - \delta_{\sigma'_2 \sigma_1} \delta_{\sigma'_1 \sigma_2} (\delta_{\omega'_2, \omega_1 + \Omega_1} + \delta_{\omega'_1, \omega_2 + \Omega_2})] + (\Omega_1 \leftrightarrow \Omega_2) \right\}. \quad (2.7)$$

For later reference let us also calculate the site-averaged mixed six-point vertex

$$\Gamma_0^{\bar{c}\bar{c}cc\phi\phi}(\sigma'_1 \omega'_1, \sigma'_2 \omega'_2; \sigma_2 \omega_2, \sigma_1 \omega_1; \Omega_1, \Omega_2) = \frac{1}{N^2 M} \sum_{n_1, n_2=1}^N \sum_{k=1}^M \Gamma_0^{\bar{c}\bar{c}cc\phi\phi}(n_1 \sigma'_1 \omega'_1, n_2 \sigma'_2 \omega'_2; n_2 \sigma_2 \omega_2, n_1 \sigma_1 \omega_1; k \Omega_1, k \Omega_2). \quad (2.8)$$

Actually, for our purpose we only need this vertex in the limit of large N and M where only the terms involving $\delta_{n'_1, n_1} \delta_{n'_2, n_2}$ in Eq. (2.7) contribute,

$$\Gamma_0^{\bar{c}\bar{c}cc\phi\phi}(\sigma'_1 \omega'_1, \sigma'_2 \omega'_2; \sigma_2 \omega_2, \sigma_1 \omega_1; \Omega_1, \Omega_2) = \frac{\beta}{2} (g_1^2 + g_2^2) \delta_{\sigma'_1, \sigma_1} \delta_{\sigma'_2, \sigma_2} (\delta_{\omega'_2, \omega_1 + \Omega_1} + \delta_{\omega'_1, \omega_2 + \Omega_2}) + (\Omega_1 \leftrightarrow \Omega_2) + \mathcal{O}(1/N). \quad (2.9)$$

To derive formally exact FRG flow equations for the irreducible vertices of the model defined by the bare action $S_2 + S_6$ in Eqs. (1.2) and (2.6) we add frequency-dependent

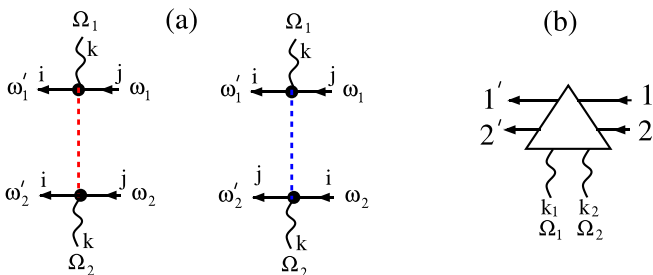


FIG. 1. (a) Graphical representation of the bare interaction vertices in the bare action S_6 given in Eq. (2.6). Outgoing arrows represent $\bar{c}_{i\sigma\omega}$, incoming arrows represent $c_{i\sigma\omega}$, wavy external lines represent $\phi_{k\Omega}$, the red-dashed line represents the bare interaction vertex $g_1^2 - g_2^2$ while the blue-dashed line represents $g_1^2 + g_2^2$. Note that on both ends of the dashed lines the frequencies are separately conserved. (b) Graphical representation of the (anti)symmetrized bare interaction vertex $\Gamma_0^{\bar{c}\bar{c}cc\phi\phi}(1', 2'; 2, 1; k_1 \Omega_1, k_2 \Omega_2)$ in Eq. (2.6).

regulators $R_\Lambda(\omega)$ and $R_\Lambda^\phi(\Omega)$ to the quadratic part of the action, where the cutoff-parameter Λ should be chosen such that the regulators vanish for $\Lambda = 0$ and diverge for $\Lambda \rightarrow \infty$. At this point it is not necessary to specify the regulators. The modified quadratic part of the Euclidean action is then

$$S_{2,\Lambda} = -\frac{1}{\beta} \sum_{n\sigma\omega} G_{0,\Lambda}^{-1}(\omega) \bar{c}_{n\sigma\omega} c_{n\sigma\omega} \\ + \frac{1}{2\beta} \sum_{k\Omega} F_{0,\Lambda}^{-1}(\Omega) \phi_{k\Omega}^* \phi_{k\Omega}, \quad (2.10)$$

where we have introduced the regularized inverse propagators

$$G_{0,\Lambda}^{-1}(\omega) = i\omega + \mu - R_\Lambda(\omega), \quad (2.11)$$

$$F_{0,\Lambda}^{-1}(\Omega) = |\Omega| + \Delta + R_\Lambda^\phi(\Omega). \quad (2.12)$$

To obtain the flow equation for the generating functional of the irreducible vertices of the YSYK model for finite N and M we introduce the cutoff-dependent generating functional of the connected imaginary time correlation functions,

$$e^{\mathcal{G}_\Lambda[\bar{c}, c, \phi]} = \frac{\int \mathcal{D}[\bar{c}, c, \phi] e^{-S_{2,\Lambda} - S_6 + (\bar{c}, c) + (\bar{c}, j) + (J, \phi)}}{\int \mathcal{D}[\bar{c}, c, \phi] e^{-S_{2,\Lambda}}}, \quad (2.13)$$

where $\bar{j}_{n\sigma\omega}$ and $j_{n\sigma\omega}$ are independent Grassmann sources, $J_{k\Omega}$ is a bosonic source, and we have introduced the notations

$$(\bar{j}, c) + (\bar{c}, j) = \frac{1}{\beta} \sum_{n\sigma\omega} [\bar{j}_{n\sigma\omega} c_{n\sigma\omega} + \bar{c}_{n\sigma\omega} j_{n\sigma\omega}], \quad (2.14)$$

$$(J, \phi) = \frac{1}{\beta} \sum_{k\Omega} J_{k\Omega}^* \phi_{k\Omega}. \quad (2.15)$$

The generating functional of the irreducible vertices (average effective action) can now be defined via the subtracted Legendre transform

$$\begin{aligned} \Gamma_\Lambda[\langle\bar{c}\rangle, \langle c\rangle, \langle\phi\rangle] &= (\bar{j}, \langle c\rangle) + (\langle\bar{c}\rangle, j) + (J, \langle\phi\rangle) - \mathcal{G}_\Lambda[\bar{j}, j, J] \\ &\quad - \frac{1}{\beta} \sum_{n\sigma\omega} R_\Lambda(\omega) \langle\bar{c}_{n\sigma\omega}\rangle \langle c_{n\sigma\omega}\rangle \\ &\quad - \frac{1}{2\beta} \sum_{k\Omega} R_\Lambda^\phi(\Omega) \langle\phi_{k\Omega}^*\rangle \langle\phi_{k\Omega}\rangle, \end{aligned} \quad (2.16)$$

where on the right-hand side the sources \bar{j} and j should be expressed in terms of the source-dependent expectation values $\langle\bar{c}\rangle$, $\langle c\rangle$, and $\langle\phi\rangle$ by inverting the relations

$$\langle c_{n\sigma\omega}\rangle = \frac{\delta \mathcal{G}_\Lambda[\bar{j}, j, J]}{\delta \bar{j}_{n\sigma\omega}}, \quad (2.17a)$$

$$\langle\bar{c}_{n\sigma\omega}\rangle = -\frac{\delta \mathcal{G}_\Lambda[\bar{j}, j, J]}{\delta j_{n\sigma\omega}}, \quad (2.17b)$$

$$\langle\phi_{k\Omega}\rangle = \frac{\delta \mathcal{G}_\Lambda[\bar{j}, j, J]}{\delta J_{k\Omega}^*}. \quad (2.17c)$$

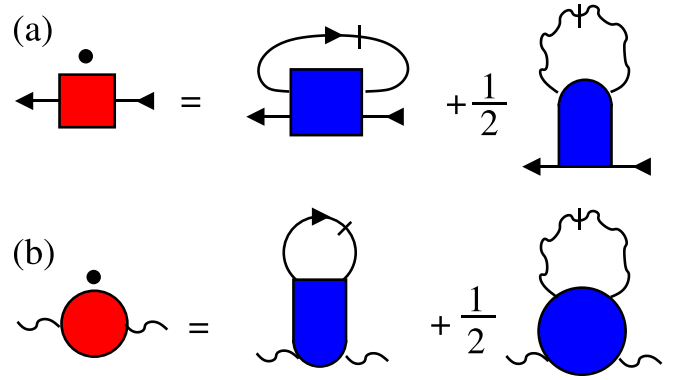


FIG. 2. Graphical representation of the exact FRG flow equations for the irreducible two-point vertices: (a) flow equation (2.22) of the fermionic self-energy; (b) flow equation (2.23) of the bosonic self-energy. The dot above the vertices on the left-hand side represents the scale derivative ∂_Λ . Outgoing arrows represent external legs associated with \bar{c} while incoming arrows represent c . The external wavy lines correspond to ϕ . Slashed lines with arrows represent the fermion single-scale propagator $\hat{G}_\Lambda(\omega)$, while slashed wavy lines represent the boson single-scale propagator $\hat{F}_\Lambda(\Omega)$. The blue symbols represent three different types of four-point vertices distinguished by the external legs.

The functional $\Gamma_\Lambda[\langle\bar{c}\rangle, \langle c\rangle, \langle\phi\rangle]$ satisfies the usual Wetterich equation [19–22] for systems involving both bosonic and fermionic fields [14]. For notational simplicity we will now rename $\langle\bar{c}\rangle \rightarrow \bar{c}$, $\langle c\rangle \rightarrow c$ and $\langle\phi\rangle \rightarrow \phi$, i.e., the symbols \bar{c} , c , and ϕ now denote the expectation values of the corresponding quantum fields in the presence of sources. For finite N and M the first few terms in the vertex expansion of the functional $\Gamma_\Lambda[\bar{c}, c, \phi]$ then have the following structure,

$$\begin{aligned} \Gamma_\Lambda[\bar{c}, c, \phi] &= \beta\Omega_\Lambda + \frac{1}{\beta} \sum_{n'n\sigma\omega} [-\delta_{nn'}(i\omega + \mu) + \Sigma_\Lambda^{n'n}(\omega)] \bar{c}_{n'\sigma\omega} c_{n\sigma\omega} + \frac{1}{2\beta} \sum_{k'\Omega} [\delta_{kk'}(|\Omega| + \Delta) + \Pi_\Lambda^{k'k}(\Omega)] \phi_{k'\Omega}^* \phi_{k\Omega} \\ &\quad + \frac{1}{(2!)^2 N \beta^4} \sum_{n'_1 n'_2 n_1} \sum_{\sigma'_1 \sigma'_2 \sigma_1} \sum_{\omega'_1 \omega'_2 \omega_1} \beta \delta_{\omega'_1 + \omega'_2, \omega_2 + \omega_1} \Gamma_\Lambda^{\bar{c}c c c}(1', 2'; 2, 1) \bar{c}_{n'_1 \sigma'_1 \omega'_1} \bar{c}_{n'_2 \sigma'_2 \omega'_2} c_{n_2 \sigma_2 \omega_2} c_{n_1 \sigma_1 \omega_1} \\ &\quad + \frac{1}{4! M \beta^4} \sum_{k_1 k_2 k_3 k_4} \sum_{\Omega_1 \dots \Omega_4} \beta \delta_{\Omega_1 + \Omega_2 + \Omega_3 + \Omega_4, 0} \Gamma_\Lambda^{\phi \phi \phi \phi}(k_1 \Omega_1, k_2 \Omega_2, k_3 \Omega_3, k_4 \Omega_4) \phi_{k_1 \Omega_1} \phi_{k_2 \Omega_2} \phi_{k_3 \Omega_3} \phi_{k_4 \Omega_4} \\ &\quad + \frac{1}{2! M \beta^4} \sum_{n'n k_1 k_2} \sum_{\sigma \omega' \omega \Omega_1 \Omega_2} \beta \delta_{\omega', \omega + \Omega_1 + \Omega_2} \Gamma_\Lambda^{\bar{c} c \phi \phi}(n' \sigma \omega'; n \sigma \omega; k_1 \Omega_1, k_2 \Omega_2) \bar{c}_{n' \sigma \omega'} c_{n \sigma \omega} \phi_{k_1 \Omega_1} \phi_{k_2 \Omega_2} \\ &\quad + \frac{1}{(2!)^3 N M \beta^6} \sum_{n'_1 n'_2 n_1} \sum_{\sigma'_1 \sigma'_2 \sigma_1} \sum_{\omega'_1 \omega'_2 \omega_1} \sum_{k_1 k_2} \sum_{\Omega_1 \Omega_2} \beta \delta_{\omega'_1 + \omega'_2, \omega_2 + \omega_1 + \Omega_1 + \Omega_2} \Gamma_\Lambda^{\bar{c} c c c \phi \phi}(1', 2'; 2, 1; k_1 \Omega_1, k_2 \Omega_2) \\ &\quad \times \bar{c}_{n'_1 \sigma'_1 \omega'_1} \bar{c}_{n'_2 \sigma'_2 \omega'_2} c_{n_2 \sigma_2 \omega_2} c_{n_1 \sigma_1 \omega_1} \phi_{k_1 \Omega_1} \phi_{k_2 \Omega_2}, + \dots, \end{aligned} \quad (2.18)$$

where in the arguments of the fermionic four-point vertex and in the six-point vertex we have abbreviated $n_1 \sigma_1 \omega_1 \rightarrow 1$ and similarly for the other fermionic labels, and we have omitted other six-point vertices involving different field combinations as well as vertices involving more than six fields.

Using the general flow equations generated by the vertex expansion of the Wetterich equation given in Ref. [14], we may now write down formally exact flow equations for vertices in the above expansion for finite N and M . The scale-dependent grand

canonical potential satisfies the exact flow equation

$$\partial_\Lambda \Omega_\Lambda = \frac{1}{\beta} \sum_{n\sigma\omega} G_\Lambda^{nn}(\omega) \partial_\Lambda R_\Lambda(\omega) + \frac{1}{2\beta} \sum_{k\Omega} F_\Lambda^{kk}(\Omega) \partial_\Lambda R_\Lambda^\phi(\Omega), \quad (2.19)$$

where $G_\Lambda^{nn}(\omega)$ and $F_\Lambda^{kk}(\Omega)$ are the diagonal elements of the scale-dependent propagator matrices whose inverse is given by the following matrices in the flavor indices,

$$[\mathbf{G}_\Lambda^{-1}(\omega)]^{nn'} = \delta_{nn'}[i\omega + \mu - R_\Lambda(\omega)] - \Sigma_\Lambda^{nn'}(\omega), \quad (2.20)$$

$$[\mathbf{F}_\Lambda^{-1}(\Omega)]^{kk'} = \delta_{kk'}[|\Omega| + \Delta + R_\Lambda^\phi(\Omega)] + \Pi_\Lambda^{kk'}(\Omega). \quad (2.21)$$

The irreducible fermionic self-energy $\Sigma_\Lambda^{nn'}(\omega)$ satisfies the exact flow equation

$$\partial_\Lambda \Sigma_\Lambda^{nn'}(\omega) = \frac{1}{N\beta} \sum_{mm'} \sum_{\sigma'\omega'} \dot{G}_\Lambda^{mm'}(\omega') \Gamma_\Lambda^{\bar{c}\bar{c}cc}(n\sigma\omega, m\sigma'\omega'; m'\sigma'\omega', n'\sigma\omega) + \frac{1}{2M\beta} \sum_{kk'} \sum_{\Omega} \dot{F}_\Lambda^{kk'}(\Omega) \Gamma_\Lambda^{\bar{c}c\phi\phi}(n\sigma\omega; n'\sigma\omega; k\bar{\Omega}, k'\Omega), \quad (2.22)$$

while the scale-dependent bosonic self-energy satisfies

$$\partial_\Lambda \Pi_\Lambda^{kk'}(\Omega) = \frac{1}{M\beta} \sum_{nn'} \sum_{\sigma\omega} \dot{G}_\Lambda^{nn'}(\omega) \Gamma_\Lambda^{\bar{c}c\phi\phi}(n\sigma\omega; n'\sigma\omega; k\bar{\Omega}, k'\Omega) + \frac{1}{2M\beta} \sum_{ll'} \sum_{\Omega'} \dot{F}_\Lambda^{ll'}(\Omega') \Gamma_\Lambda^{\phi\phi\phi\phi}(l\bar{\Omega}', l'\Omega', k\bar{\Omega}, k'\Omega), \quad (2.23)$$

where we have introduced the abbreviation $\bar{\Omega} = -\Omega$ and $\dot{G}_\Lambda^{nn'}(\omega)$ and $\dot{F}_\Lambda^{kk'}(\Omega)$ are the fermionic and bosonic single-scale propagators [14]. Graphical representations of the flow equations (2.22) and (2.23) are shown in Fig. 2. The right-hand sides of these flow equations depend on three different types of four-point vertices, which in turn satisfy flow equations involving not only four-point vertices but also various types of six-point vertices. For example, the exact flow equation for the fermionic four-point vertex is

$$\begin{aligned} \partial_\Lambda \Gamma_\Lambda^{\bar{c}\bar{c}cc}(n'_1\sigma'_1\omega'_1, n'_2\sigma'_2\omega'_2; n_2\sigma_2\omega_2, n_1\sigma_1\omega_1) &= \frac{1}{N\beta} \sum_{nn'} \sum_{\sigma\omega} \dot{G}_\Lambda^{nn'}(\omega) \Gamma_\Lambda^{\bar{c}\bar{c}cccc}(1', 2', n\sigma\omega; n'\sigma\omega, 2, 1) \\ &+ \frac{1}{2M\beta} \sum_{kk'} \sum_{\Omega} \dot{F}_\Lambda^{kk'}(\Omega) \Gamma_\Lambda^{\bar{c}\bar{c}c\phi\phi}(1', 2'; 2, 1; k\bar{\Omega}, k'\Omega) \\ &+ L_\Lambda^{\text{pp}}(1', 2'; 2, 1) + L_\Lambda^{\text{ph}}(1', 2'; 2, 1) + L_\Lambda^{\text{bos}}(1', 2'; 2, 1), \end{aligned} \quad (2.24)$$

where on the right-hand side we have used again the abbreviation $1 = (n_1\sigma_1\omega_1)$, and in the last line we have introduced three different loop contributions,

$$\begin{aligned} L_\Lambda^{\text{pp}}(1', 2'; 2, 1) &= -\frac{1}{N^2\beta} \sum_{nn'} \sum_{mm'} \sum_{\sigma\sigma'} \sum_{\omega} \dot{G}_\Lambda^{nn'}(\omega) G_\Lambda^{mm'}(\omega_1 + \omega_2 - \omega) \Gamma_\Lambda^{\bar{c}\bar{c}cc}(1', 2'; n\sigma'\omega_1 + \omega_2 - \omega, m\sigma\omega) \\ &\times \Gamma_\Lambda^{\bar{c}\bar{c}cc}(m'\sigma\omega, n'\sigma'\omega_1 + \omega_2 - \omega; 2, 1), \end{aligned} \quad (2.25)$$

$$\begin{aligned} L_\Lambda^{\text{ph}}(1', 2'; 2, 1) &= \frac{1}{N^2\beta} \sum_{nn'} \sum_{mm'} \sum_{\sigma\sigma'} \sum_{\omega} [\dot{G}_\Lambda^{nn'}(\omega) G_\Lambda^{mm'}(\omega + \omega_1 - \omega'_1) + G_\Lambda^{nn'}(\omega) \dot{G}_\Lambda^{mm'}(\omega + \omega_1 - \omega'_1)] \\ &\times \Gamma_\Lambda^{\bar{c}\bar{c}cc}(1', m'\sigma'\omega + \omega_1 - \omega'_1; n\sigma\omega, 1) \Gamma_\Lambda^{\bar{c}\bar{c}cc}(2', n'\sigma\omega; m\sigma'\omega + \omega_1 - \omega'_1, 2) - \{(n_1\sigma_1\omega_1) \leftrightarrow (n_2\sigma_2\omega_2)\}, \end{aligned} \quad (2.26)$$

$$\begin{aligned} L_\Lambda^{\text{bos}}(1', 2'; 2, 1) &= -\frac{1}{M^2\beta} \sum_{kk'} \sum_{ll'} \sum_{\Omega} \dot{F}_\Lambda^{kk'}(\Omega) F_\Lambda^{ll'}(\Omega + \omega_1 - \omega'_1) \\ &\times \Gamma_\Lambda^{\bar{c}c\phi\phi}(1'; 1; k\Omega, l\bar{\Omega} - \omega_1 + \omega'_1) \Gamma_\Lambda^{\bar{c}c\phi\phi}(2'; 2; k'\bar{\Omega}, l'\Omega - \omega_2 + \omega'_2) + \{(n_1\sigma_1\omega_1) \leftrightarrow (n_2\sigma_2\omega_2)\}. \end{aligned} \quad (2.27)$$

A graphical representation of the exact flow equation (2.24) for the fermionic four-point vertex is shown in Fig. 3. The six-point vertices on the right-hand side of Eq. (2.24) satisfy flow equations involving various types of eight-point vertices.

Obviously, for finite N and M the FRG vertex expansion generates an infinite hierarchy of flow equations.

The crucial point is now that in the limit $N \rightarrow \infty$ and $M \rightarrow \infty$ the system of flow equations can be closed to leading order

in $1/N$ and $1/M$ where we can retain only the contributions to the flow equations, which have finite limits for $N \rightarrow \infty$ and $M \rightarrow \infty$. The self-energies are then diagonal in the site indices,

$$\Sigma_{\Lambda}^{nn'}(\omega) = \delta_{nn'} \Sigma_{\Lambda}(\omega) + \mathcal{O}(1/N), \quad (2.28)$$

$$\Pi_{\Lambda}^{kk'}(\Omega) = \delta_{kk'} \Pi_{\Lambda}(\Omega) + \mathcal{O}(1/N), \quad (2.29)$$

where the symbol $\mathcal{O}(1/N)$ represents also terms of order $1/M$ because we assume that the ratio N/M is of order

unity. The leading large- N limit of the four-point vertices is more complicated. Consider first the fermionic four-point vertex $\Gamma_{\Lambda}^{\bar{c}c\bar{c}c}(n'_1\sigma'_1\omega'_1, n'_2\sigma'_2\omega'_2; n_2\sigma_2\omega_2, n_1\sigma_1\omega_1)$. We obtain a consistent large- N truncation of the hierarchy of FRG flow equations if we assume that the leading components of the fermionic four-point vertex are constrained by the condition that site labels n'_1 and n'_2 of the two outgoing fermions agree with the site labels n_1 and n_2 of the two incoming fermions up to a permutation. Taking into account the antisymmetry of $\Gamma_{\Lambda}^{\bar{c}c\bar{c}c}(1', 2'; 2, 1)$ with respect to the exchange $1' \leftrightarrow 2'$ and $1 \leftrightarrow 2$, this implies

$$\begin{aligned} \Gamma_{\Lambda}^{\bar{c}c\bar{c}c}(n'_1\sigma'_1\omega'_1, n'_2\sigma'_2\omega'_2; n_2\sigma_2\omega_2, n_1\sigma_1\omega_1) &= \delta_{n'_1n_1}\delta_{n'_2n_2}\Gamma_{\Lambda}^{\bar{c}c\bar{c}c}(\sigma'_1\omega'_1, \sigma'_2\omega'_2; \sigma_2\omega_2, \sigma_1\omega_1) \\ &\quad - \delta_{n'_1n_2}\delta_{n'_2n_1}\Gamma_{\Lambda}^{\bar{c}c\bar{c}c}(\sigma'_2\omega'_2, \sigma'_1\omega'_1; \sigma_2\omega_2, \sigma_1\omega_1) + \mathcal{O}(1/N), \end{aligned} \quad (2.30)$$

where

$$\Gamma_{\Lambda}^{\bar{c}c\bar{c}c}(\sigma'_1\omega'_1, \sigma'_2\omega'_2; \sigma_2\omega_2, \sigma_1\omega_1) = \lim_{N \rightarrow \infty} \Gamma_{\Lambda}^{\bar{c}c\bar{c}c}(n_1\sigma'_1\omega'_1, n_2\sigma'_2\omega'_2; n_2\sigma_2\omega_2, n_1\sigma_1\omega_1). \quad (2.31)$$

Note that to leading order in $1/N$ the fermionic four-point vertex gives the following contribution to the vertex expansion of the average effective action defined in Eq. (2.18),

$$\begin{aligned} &\frac{1}{(2!)^2 N \beta^4} \sum_{n'_1 n'_2 n_1 n_2} \sum_{\sigma'_1 \sigma'_2 \sigma_1 \sigma_2} \sum_{\omega'_1 \omega'_2 \omega_1 \omega_2} \beta \delta_{\omega'_1 + \omega'_2, \omega_2 + \omega_1} \Gamma_{\Lambda}^{\bar{c}c\bar{c}c}(1', 2'; 2, 1) \bar{c}_{n'_1 \sigma'_1 \omega'_1} \bar{c}_{n'_2 \sigma'_2 \omega'_2} c_{n_2 \sigma_2 \omega_2} c_{n_1 \sigma_1 \omega_1} \\ &\approx \frac{N}{2! \beta^4} \sum_{\sigma'_1 \sigma'_2 \sigma_1 \sigma_2} \sum_{\omega'_1 \omega'_2 \omega_1 \omega_2} \beta \delta_{\omega'_1 + \omega'_2, \omega_2 + \omega_1} \Gamma_{\Lambda}^{\bar{c}c\bar{c}c}(\sigma'_1 \omega'_1, \sigma'_2 \omega'_2; \sigma_2 \omega_2, \sigma_1 \omega_1) \Psi_{\sigma'_1 \omega'_1 \sigma_1 \omega_1} \Psi_{\sigma'_2 \omega'_2 \sigma_2 \omega_2}, \end{aligned} \quad (2.32)$$

where we have introduced the site-averaged composite field

$$\Psi_{\sigma' \omega' \sigma \omega} = \frac{1}{N} \sum_n \bar{c}_{n \sigma' \omega'} c_{n \sigma \omega}. \quad (2.33)$$

This field resembles the collective Hubbard-Stratonovich field introduced in the path integral derivation of the Dyson-Schwinger equations from the large- N saddle point [1, 11, 12]. However, in Eq. (2.33) the symbols $\bar{c}_{n \sigma' \omega'}$ and $c_{n \sigma \omega}$ represent the source-dependent expectation values of the corresponding Grassmann fields, so that the above $\Psi_{\sigma' \omega' \sigma \omega}$ cannot be identified with the Hubbard-Stratonovich field introduced in the path integral approach.

To solve our flow equations for the two-point vertices for large N we also need the leading large- N limit of the mixed four-point vertex,

$$\begin{aligned} &\Gamma_{\Lambda}^{\bar{c}c\phi\phi}(n'\sigma\omega'; n\sigma\omega; k_1\Omega_1, k_2\Omega_2) \\ &= \delta_{n'n} \delta_{k_1 k_2} \Gamma_{\Lambda}^{\bar{c}c\phi\phi}(\sigma\omega'; \sigma\omega; \Omega_1, \Omega_2) + \mathcal{O}(1/N), \end{aligned} \quad (2.34)$$

where

$$\Gamma_{\Lambda}^{\bar{c}c\phi\phi}(\sigma\omega'; \sigma\omega; \Omega_1, \Omega_2) = \lim_{N \rightarrow \infty} \Gamma_{\Lambda}^{\bar{c}c\phi\phi}(n\sigma\omega'; n\sigma\omega; k\Omega_1, k\Omega_2). \quad (2.35)$$

Finally, the purely bosonic four-point vertex has for large N the form

$$\begin{aligned} &\Gamma_{\Lambda}^{\phi\phi\phi\phi}(k_1\Omega_1, k_2\Omega_2, k_3\Omega_3, k_4\Omega_4) \\ &= \delta_{k_1 k_2} \delta_{k_3 k_4} \Gamma_{\Lambda}^{\phi\phi\phi\phi}(\Omega_1, \Omega_2, \Omega_3, \Omega_4) \\ &\quad + \delta_{k_1 k_3} \delta_{k_2 k_4} \Gamma_{\Lambda}^{\phi\phi\phi\phi}(\Omega_1, \Omega_3, \Omega_2, \Omega_4) \\ &\quad + \delta_{k_1 k_4} \delta_{k_2 k_3} \Gamma_{\Lambda}^{\phi\phi\phi\phi}(\Omega_1, \Omega_4, \Omega_2, \Omega_3) + \mathcal{O}(1/N), \end{aligned} \quad (2.36)$$

with

$$\begin{aligned} &\Gamma_{\Lambda}^{\phi\phi\phi\phi}(\Omega_1, \Omega_2, \Omega_3, \Omega_4) \\ &= \lim_{N \rightarrow \infty} \Gamma_{\Lambda}^{\phi\phi\phi\phi}(k_1\Omega_1, k_1\Omega_2, k_2\Omega_3, k_2\Omega_4). \end{aligned} \quad (2.37)$$

It turns out that the bosonic four-point vertex does not contribute to the flow of the two-point vertices to leading order in $1/N$ because this vertex vanishes in the bare action and is not generated by the FRG flow to this order.

It is now easy to see that the loop contributions L_{Λ}^{pp} , L_{Λ}^{ph} , and L_{Λ}^{bos} defined in Eqs. (2.25)–(2.27) do not contribute to the flow of the fermionic four-point vertex to leading order in $1/N$ [23]. Consider first the particle-particle loop $L_{\Lambda}^{\text{pp}}(1', 2'; 2, 1)$ in Eq. (2.25) for the relevant index combinations $n'_1 = n_1, n'_2 = n_2$ or $n'_1 = n_2, n'_2 = n_1$. Keeping in mind that for large N the propagators are diagonal in the flavor indices, we see that the flavor sums in Eq. (2.25) collapses to $2 = \mathcal{O}(1)$ terms, so that $L_{\Lambda}^{\text{pp}}(1', 2'; 2, 1) = \mathcal{O}(1/N^2)$. Moreover, in $L_{\Lambda}^{\text{ph}}(1', 2'; 2, 1)$ and $L_{\Lambda}^{\text{bos}}(1', 2'; 2, 1)$ only one of the flavor sums collapses, so that these contributions are of order $1/N$. By the same argument, the leading large- N contribution in the FRG flow equations for any n -point vertex is given by the term where two legs of the $(n+2)$ -point vertex are joined by a single propagator line. In the flow equations for the four-point vertices, we therefore have to consider only the contributions from the six-point vertices. Given the fact that the bare action S_6 given in Eq. (2.6) depends only on the mixed six-point vertex $\Gamma_{\Lambda}^{\bar{c}c\phi\phi\phi\phi}$ with initial value given in Eq. (2.7), to leading order in $1/N$ we can neglect the FRG flow of all other six-point vertices. If we insert this initial value on the right-hand side of the flow equation

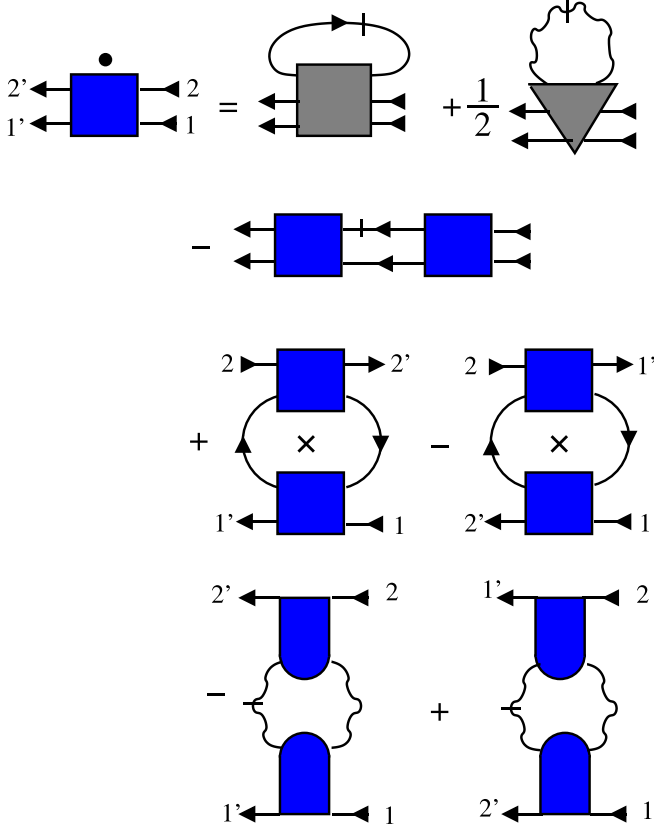


FIG. 3. Graphical representation of the exact FRG flow equation (2.24) for the fermionic four-point vertex. The gray square represents the fermionic six-point vertex, while the gray triangle represents the mixed six-point vertex with four fermionic and two bosonic external legs. The internal lines with arrows represent the exact scale-dependent fermion propagator $G_\Lambda(\omega)$, whereas wavy internal lines represent the boson propagator $F_\Lambda(\Omega)$. The cross inside the loops means that one should sum up two diagrams where either the right or the left propagator forming the loop is replaced by the corresponding single-scale propagator. The rest of the symbols is defined in the caption of Fig. 2.

(2.24), we see that only the site-average of the six-point vertex given in Eq. (2.9) contributes. Moreover, following the analysis of the diagrams in the flow equation for the fermionic four-point vertex presented in the paragraph after Eq. (2.24), and using the fact that the bare action does not contain any eight-point vertices, we see that to leading order in $1/N$ the mixed six-point vertex is not renormalized. We thus arrive at the following large- N truncation of the formally exact FRG flow equations for the YSYK model: The flow of the site-diagonal two-point vertices is related to the large- N limits of four-point vertices defined in Eqs. (2.31) and (2.35) as follows,

$$\begin{aligned} \partial_\Lambda \Sigma_\Lambda(\omega) &= \frac{1}{\beta} \sum_{\sigma'\omega'} \dot{G}_\Lambda(\omega') \Gamma_\Lambda^{\bar{c}c c c}(\sigma\omega, \sigma'\omega'; \sigma'\omega', \sigma\omega) \\ &+ \frac{1}{2\beta} \sum_{\Omega} \dot{F}_\Lambda(\Omega) \Gamma_\Lambda^{\bar{c}c\phi\phi}(\sigma\omega; \sigma\omega; -\Omega, \Omega), \end{aligned} \quad (2.38)$$

$$\partial_\Lambda \Pi_\Lambda(\Omega) = \frac{N}{M\beta} \sum_{\sigma\omega} \dot{G}_\Lambda(\omega) \Gamma_\Lambda^{\bar{c}c\phi\phi}(\sigma\omega; \sigma\omega; -\Omega, \Omega), \quad (2.39)$$

where the single-scale propagators are

$$\dot{G}_\Lambda(\omega) = -G_\Lambda^2(\omega) \partial_\Lambda G_{0,\Lambda}^{-1}(\omega) = G_\Lambda^2(\omega) \partial_\Lambda R_\Lambda(\omega), \quad (2.40)$$

$$\dot{F}_\Lambda(\Omega) = -F_\Lambda^2(\Omega) \partial_\Lambda F_{0,\Lambda}^{-1}(\Omega) = -F_\Lambda^2(\Omega) \partial_\Lambda R_\Lambda^\phi(\Omega), \quad (2.41)$$

and the scale-dependent propagators are related to the corresponding self-energies via the regularized Dyson equations

$$\begin{aligned} G_\Lambda(\omega) &= \frac{1}{G_{0,\Lambda}^{-1}(\omega) - \Sigma_\Lambda(\omega)} \\ &= \frac{1}{i\omega + \mu - R_\Lambda(\omega) - \Sigma_\Lambda(\omega)}, \end{aligned} \quad (2.42)$$

$$\begin{aligned} F_\Lambda(\Omega) &= \frac{1}{F_{0,\Lambda}^{-1}(\Omega) + \Pi_\Lambda(\Omega)} \\ &= \frac{1}{|\Omega| + \Delta + R_\Lambda^\phi(\Omega) + \Pi_\Lambda(\Omega)}. \end{aligned} \quad (2.43)$$

The four-point vertices on the right-hand side of the flow equations (2.38) and (2.39) for the two-point vertices satisfy

$$\begin{aligned} \partial_\Lambda \Gamma_\Lambda^{\bar{c}c c c}(\sigma'_1\omega'_1, \sigma'_2\omega'_2; \sigma_2\omega_2, \sigma_1\omega_1) \\ = \frac{1}{2\beta} \sum_{\Omega} \dot{F}_\Lambda(\Omega) \Gamma_0^{\bar{c}c c c\phi\phi} \\ \times (\sigma'_1\omega'_1, \sigma'_2\omega'_2; \sigma_2\omega_2, \sigma_1\omega_1; -\Omega, \Omega), \end{aligned} \quad (2.44)$$

and

$$\begin{aligned} \partial_\Lambda \Gamma_\Lambda^{\bar{c}c\phi\phi}(\sigma'\omega'; \sigma\omega; \Omega_1, \Omega_2) \\ = \frac{1}{\beta} \sum_{\sigma_1\omega_1} \dot{G}_\Lambda(\omega_1) \Gamma_0^{\bar{c}c c c\phi\phi} \\ \times (\sigma'\omega', \sigma_1\omega_1; \sigma_1\omega_1, \sigma\omega; \Omega_1, \Omega_2), \end{aligned} \quad (2.45)$$

where the large- N limit of the initial value of the site-averaged mixed six-point vertex $\Gamma_0^{\bar{c}c c c\phi\phi}(\dots)$ is given in Eq. (2.9). A graphical representation of the above large- N truncation of the FRG flow equations is shown in Fig. 4. Substituting our explicit expression (2.9) for the initial value of the site-averaged six-point vertex into Eqs. (2.44) and (2.45), we see that the fermionic four-point vertex in the flow equation (2.38) is spin-diagonal while the mixed four-point vertex in Eq. (2.39) is actually independent of the spin label σ so that we can write

$$\Gamma_\Lambda^{\bar{c}c c c}(\sigma\omega, \sigma'\omega'; \sigma'\omega', \sigma\omega) = \delta_{\sigma\sigma'} \Gamma_\Lambda^{\bar{c}c c c}(\omega, \omega'; \omega', \omega), \quad (2.46)$$

$$\Gamma_\Lambda^{\bar{c}c\phi\phi}(\sigma\omega; \sigma\omega; -\Omega, \Omega) = \Gamma_\Lambda^{\bar{c}c\phi\phi}(\omega; \omega; -\Omega, \Omega). \quad (2.47)$$

With this notation the flow equations (2.38, 2.39) for the self-energies can be written as

$$\begin{aligned} \partial_\Lambda \Sigma_\Lambda(\omega) &= \frac{1}{\beta} \sum_{\omega'} \dot{G}_\Lambda(\omega') \Gamma_\Lambda^{\bar{c}c c c}(\omega, \omega'; \omega', \omega) \\ &+ \frac{1}{2\beta} \sum_{\Omega} \dot{F}_\Lambda(\Omega) \Gamma_\Lambda^{\bar{c}c\phi\phi}(\omega; \omega; -\Omega, \Omega), \end{aligned} \quad (2.48)$$

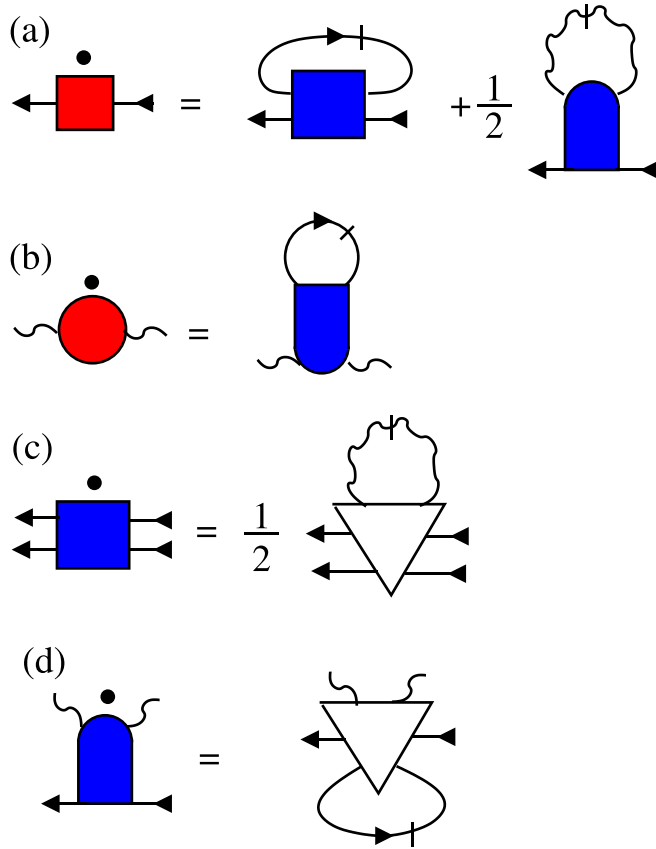


FIG. 4. Graphical representation of our large- N truncation of the hierarchy of FRG flow equations for the YSYK model. (a) Fermionic self-energy, Eq. (2.38); (b) bosonic self-energy, Eq. (2.39); (c) fermionic four-point vertex, Eq. (2.44); and (d) mixed four-point vertex, Eq. (2.45). The empty triangle represents the large- N limit of the symmetrized bare six-point vertex given in Eq. (2.9).

$$\partial_\Lambda \Pi_\Lambda(\Omega) = \frac{p}{\beta} \sum_{\omega} \dot{G}_\Lambda(\omega) \Gamma_\Lambda^{\bar{c}c\phi\phi}(\omega; \omega; -\Omega, \Omega), \quad (2.49)$$

while the flow of the scale-dependent four-point vertices is

$$\partial_\Lambda \Gamma_\Lambda^{\bar{c}c\bar{c}c}(\omega, \omega'; \omega', \omega) = g^2 \dot{F}_\Lambda(\omega - \omega'), \quad (2.50)$$

$$\partial_\Lambda \Gamma_\Lambda^{\bar{c}c\phi\phi}(\omega; \omega; -\Omega, \Omega) = g^2 [\dot{G}_\Lambda(\omega + \Omega) + \dot{G}_\Lambda(\omega - \Omega)]. \quad (2.51)$$

Here

$$g^2 = g_1^2 + g_2^2 \quad (2.52)$$

is the relevant bare coupling and we have introduced the parameter

$$p = \frac{(2S+1)N}{M} = \frac{2N}{M}, \quad (2.53)$$

where $2S+1=2$ is the spin degeneracy for spin $S=1/2$.

The four coupled flow equations (2.48)–(2.51) uniquely determine the scale-dependent fermionic and bosonic self-energies and the two relevant interaction vertices. We

emphasize that Eqs. (2.48)–(2.51) have been obtained from the formally exact hierarchy of flow equations for the irreducible vertices of the YSYK model by retaining all terms, which have a finite limit for $N \rightarrow \infty$ and $M \rightarrow \infty$.

We now show that our FRG flow equations (2.48)–(2.51) can be reduced to the usual DS equations for the self-energies of the YSYK model if we use the so-called Katanin substitution [17] to replace the single-scale propagators on the right-hand sides by the total scale derivatives of the propagators,

$$\dot{G}_\Lambda(\omega) \rightarrow \partial_\Lambda G_\Lambda(\omega) = \dot{G}_\Lambda(\omega) + G_\Lambda^2(\omega) \partial_\Lambda \Sigma_\Lambda(\omega), \quad (2.54)$$

$$\dot{F}_\Lambda(\Omega) \rightarrow \partial_\Lambda F_\Lambda(\Omega) = \dot{F}_\Lambda(\Omega) - F_\Lambda^2(\Omega) \partial_\Lambda \Pi_\Lambda(\Omega). \quad (2.55)$$

With this substitution the right-hand sides of the flow equations (2.50) and (2.51) become total Λ derivatives so that we may trivially integrate both sides over the flow parameter Λ . Taking into account that for $\Lambda_0 \rightarrow \infty$ the regularized propagators vanish we obtain

$$\Gamma_\Lambda^{\bar{c}c\bar{c}c}(\omega, \omega'; \omega', \omega) = g^2 F_\Lambda(\omega - \omega'), \quad (2.56)$$

and

$$\Gamma_\Lambda^{\bar{c}c\phi\phi}(\omega; \omega; -\Omega, \Omega) = g^2 [G_\Lambda(\omega + \Omega) + G_\Lambda(\omega - \Omega)]. \quad (2.57)$$

Substituting these equations into the flow equations (2.38) and (2.39) for the two-point functions we obtain

$$\partial_\Lambda \Sigma_\Lambda(\omega) = \frac{g^2}{\beta} \sum_{\Omega} [\dot{F}_\Lambda(\Omega) G_\Lambda(\omega - \Omega) + F_\Lambda(\Omega) \dot{G}_\Lambda(\omega - \Omega)], \quad (2.58)$$

$$\begin{aligned} \partial_\Lambda \Pi_\Lambda(\Omega) &= p \frac{g^2}{\beta} \sum_{\omega} [\dot{G}_\Lambda(\omega) G_\Lambda(\omega - \Omega) \\ &\quad + G_\Lambda(\omega) \dot{G}_\Lambda(\omega - \Omega)]. \end{aligned} \quad (2.59)$$

Using once more the Katanin substitution (2.54) and (2.55) to transform the right-hand side of the above equations into total Λ derivatives and integrating both sides over Λ we obtain for $\Lambda \rightarrow 0$ the DS equations for the YSYK model [1,6],

$$\Sigma(\omega) = \frac{g^2}{\beta} \sum_{\Omega} F(\Omega) G(\omega - \Omega), \quad (2.60)$$

$$\Pi(\Omega) = p \frac{g^2}{\beta} \sum_{\omega} G(\omega) G(\omega - \Omega). \quad (2.61)$$

We conclude that our large- N truncation of the FRG flow equations in combination with the Katanin substitution is equivalent to the DS equations obtained from the large- N saddle point of a suitably defined functional integral representation of the YSYK model. Note that without the Katanin substitution our large- N FRG flow equations are *not* equivalent to the DS equations (2.60) and (2.61) because the Katanin substitution in Eqs. (2.54) and (2.55) resums higher orders in the coupling g^2 . However, for the SYK model we have shown in Ref. [15] that the Katanin substitution does not modify the value of the fermionic anomalous dimension. Whether this is also true for the YSYK model is an interesting question beyond the scope of this paper.

III. LOW-ENERGY EXPANSION

Our aim is to determine possible fixed points of the system of FRG flow equations given in Eqs. (2.48)–(2.51) at zero temperature, $\beta^{-1} = 0$. As usual, we anticipate that the fixed points are determined by the leading low-energy behavior of the vertices, so that for our purpose it is sufficient to expand the irreducible self-energies to linear order in the frequencies. Taking the possibility of dissipative terms proportional to $|\omega|$ and $|\Omega|$ into account, the expansion is of the form

$$\Sigma_\Lambda(\omega) = \Sigma_\Lambda(0) - A_\Lambda|\omega| - (B_\Lambda - 1)i\omega + \mathcal{O}(\omega^2), \quad (3.1)$$

$$\Pi_\Lambda(\Omega) = \Pi_\Lambda(0) + (Y_\Lambda^{-1} - 1)|\Omega| + \mathcal{O}(\Omega^2), \quad (3.2)$$

where A_Λ , B_Λ , and Y_Λ are dimensionless. The coupling A_Λ parametrizes the asymmetry in the fermion spectral function, which is expected to emerge for finite values of the chemical potential μ [3]. The usual fermionic wave-function renormalization factor Z_Λ is then given by

$$Z_\Lambda = \frac{1}{\sqrt{A_\Lambda^2 + B_\Lambda^2}}, \quad (3.3)$$

which defines the scale-dependent fermionic anomalous dimension via

$$\eta_\Lambda = \frac{\Lambda \partial_\Lambda Z_\Lambda}{Z_\Lambda}. \quad (3.4)$$

Using for simplicity a sharp frequency regulator, the low-energy form of the scale-dependent fermionic propagator and the corresponding single-scale propagator can then be written as [24]

$$G_\Lambda(\omega) = \frac{Z_\Lambda \Theta(|\omega| - \Lambda)}{a_\Lambda |\omega| + ib_\Lambda \omega + \mu_\Lambda}, \quad (3.5a)$$

$$\dot{G}_\Lambda(\omega) = -\frac{Z_\Lambda \delta(|\omega| - \Lambda)}{a_\Lambda \Lambda + ib_\Lambda \Lambda \text{sgn} \omega + \mu_\Lambda}, \quad (3.5b)$$

where

$$a_\Lambda = Z_\Lambda A_\Lambda = \frac{A_\Lambda}{\sqrt{A_\Lambda^2 + B_\Lambda^2}}, \quad (3.6a)$$

$$b_\Lambda = Z_\Lambda B_\Lambda = \frac{B_\Lambda}{\sqrt{A_\Lambda^2 + B_\Lambda^2}}, \quad (3.6b)$$

and

$$\mu_\Lambda = Z_\Lambda [\mu - \Sigma_\Lambda(0)]. \quad (3.7)$$

Note that by construction $a_\Lambda^2 + b_\Lambda^2 = 1$. Similarly, using also a sharp frequency cutoff for the bosons, the bosonic propagator and the corresponding single-scale propagator are at low energies given by

$$F_\Lambda(\Omega) = \frac{Y_\Lambda \Theta(|\Omega| - \Lambda)}{|\Omega| + r_\Lambda}, \quad (3.8a)$$

$$\dot{F}_\Lambda(\Omega) = -\frac{Y_\Lambda \delta(|\Omega| - \Lambda)}{\Lambda + r_\Lambda}, \quad (3.8b)$$

where

$$r_\Lambda = Y_\Lambda [\Delta + \Pi_\Lambda(0)]. \quad (3.9)$$

The logarithmic scale dependence of the bosonic wave-function renormalization factor Y_Λ defines the scale-dependent bosonic anomalous dimension

$$\gamma_\Lambda = \frac{\Lambda \partial_\Lambda Y_\Lambda}{Y_\Lambda}. \quad (3.10)$$

For later convenience we introduce the dimensionless coupling

$$u_l = \frac{Z_l^2 Y_l g^2}{\pi \Lambda^2}, \quad (3.11)$$

which by definition satisfies the flow equation

$$\partial_l u_l = (2 - 2\eta_l - \gamma_l) u_l, \quad (3.12)$$

where $l = \ln(\Lambda_0/\Lambda)$ is the logarithmic flow parameter and $\partial_l = -\Lambda \partial_\Lambda$. From now on all quantities will be considered to be functions of l instead of Λ ; in the case of dimensionless quantities we simply rename $\eta_\Lambda \rightarrow \eta_l$, $\gamma_\Lambda \rightarrow \gamma_l$, $a_\Lambda \rightarrow a_l$ and $b_\Lambda \rightarrow b_l$, while the dimensionful couplings μ_Λ and r_Λ are divided by Λ to obtain the corresponding dimensionless rescaled couplings,

$$\mu_l = \frac{\mu_\Lambda}{\Lambda} = \frac{Z_\Lambda [\mu - \Sigma_\Lambda(0)]}{\Lambda}, \quad (3.13)$$

$$r_l = \frac{r_\Lambda}{\Lambda} = \frac{Y_\Lambda [\Delta + \Pi_\Lambda(0)]}{\Lambda}. \quad (3.14)$$

To find the fixed points of the renormalization group, we introduce the dimensionless rescaled self-energies

$$\tilde{\Sigma}_l(\tilde{\omega}) = \frac{Z_\Lambda \Sigma_\Lambda(\Lambda \tilde{\omega})}{\Lambda}, \quad (3.15)$$

$$\tilde{\Pi}_l(\tilde{\Omega}) = \frac{Y_\Lambda \Pi_\Lambda(\Lambda \tilde{\Omega})}{\Lambda}, \quad (3.16)$$

which depend on the dimensionless frequencies $\tilde{\omega} = \omega/\Lambda$ and $\tilde{\Omega} = \Omega/\Lambda$. Using the flow equations (2.48) and (2.49) for the dimensionful self-energies we find that the corresponding dimensionless rescaled quantities satisfy

$$\partial_l \tilde{\Sigma}_l(\tilde{\omega}) = (1 - \eta_l - \tilde{\omega} \partial_{\tilde{\omega}}) \tilde{\Sigma}_l(\tilde{\omega}) + \dot{\tilde{\Sigma}}_l(\tilde{\omega}), \quad (3.17)$$

$$\partial_l \tilde{\Pi}_l(\tilde{\Omega}) = (1 - \gamma_l - \tilde{\Omega} \partial_{\tilde{\Omega}}) \tilde{\Pi}_l(\tilde{\Omega}) + \dot{\tilde{\Pi}}_l(\tilde{\Omega}), \quad (3.18)$$

where

$$\begin{aligned} \dot{\tilde{\Sigma}}_l(\tilde{\omega}) &= -Z_\Lambda \partial_\Lambda \Sigma_\Lambda(\omega) \\ &= \int \frac{d\tilde{\omega}'}{2\pi} \dot{\tilde{G}}_l(\tilde{\omega}') \tilde{\Gamma}_l^{\bar{c}c\bar{c}c}(\tilde{\omega}, \tilde{\omega}'; \tilde{\omega}', \tilde{\omega}) \\ &\quad + \frac{1}{2} \int \frac{d\tilde{\Omega}}{2\pi} \dot{\tilde{F}}_l(\tilde{\Omega}) \tilde{\Gamma}_l^{\bar{c}c\phi\phi}(\tilde{\omega}, \tilde{\omega}; -\tilde{\Omega}, \tilde{\Omega}), \end{aligned} \quad (3.19)$$

$$\begin{aligned} \dot{\tilde{\Pi}}_l(\tilde{\Omega}) &= -Y_\Lambda \partial_\Lambda \Pi_\Lambda(\Omega) \\ &= p \int \frac{d\tilde{\omega}}{2\pi} \dot{\tilde{G}}_l(\tilde{\omega}) \tilde{\Gamma}_l^{\bar{c}c\phi\phi}(\tilde{\omega}, \tilde{\omega}; -\tilde{\Omega}, \tilde{\Omega}). \end{aligned} \quad (3.20)$$

Here we have introduced the dimensionless rescaled four-point vertices,

$$\tilde{\Gamma}_l^{\tilde{c}\tilde{c}cc}(\tilde{\omega}, \tilde{\omega}'; \tilde{\omega}', \tilde{\omega}) = \frac{Z_\Lambda^2}{\Lambda} \Gamma_\Lambda^{\tilde{c}\tilde{c}cc}(\Lambda\tilde{\omega}, \Lambda\tilde{\omega}'; \Lambda\tilde{\omega}', \Lambda\tilde{\omega}), \quad (3.21)$$

$$\tilde{\Gamma}_l^{\tilde{c}c\phi\phi}(\tilde{\omega}, \tilde{\omega}; -\tilde{\Omega}, \tilde{\Omega}) = \frac{Z_\Lambda Y_\Lambda}{\Lambda} \Gamma_\Lambda^{\tilde{c}c\phi\phi}(\Lambda\tilde{\omega}; \Lambda\tilde{\omega}; -\Lambda\tilde{\Omega}, \Lambda\tilde{\Omega}), \quad (3.22)$$

and the dimensionless single-scale propagators,

$$\dot{\tilde{G}}_l(\tilde{\omega}) = -\frac{\Lambda^2}{Z_\Lambda} \dot{G}_\Lambda(\Lambda\omega) \approx \frac{\delta(|\tilde{\omega}| - 1)}{a_l + ib_l \text{sgn}\omega + \mu_l}, \quad (3.23)$$

$$\dot{\tilde{F}}_l(\tilde{\omega}) = -\frac{\Lambda^2}{Y_\Lambda} \dot{F}_\Lambda(\Lambda\omega) \approx \frac{\delta(|\tilde{\Omega}| - 1)}{1 + r_l}. \quad (3.24)$$

From the flow equations (2.50) and (2.51) we obtain for the flow of the rescaled four-point vertices

$$\begin{aligned} \partial_l \tilde{\Gamma}_l^{\tilde{c}\tilde{c}cc}(\tilde{\omega}'_1, \tilde{\omega}'_2; \tilde{\omega}_2, \tilde{\omega}_1) &= (1 - 2\eta_l - \tilde{\omega}'_1 \partial_{\tilde{\omega}'_1} - \tilde{\omega}'_2 \partial_{\tilde{\omega}'_2} - \tilde{\omega}_2 \partial_{\tilde{\omega}_2} - \tilde{\omega}_1 \partial_{\tilde{\omega}_1}) \tilde{\Gamma}_l^{\tilde{c}\tilde{c}cc}(\tilde{\omega}'_1, \tilde{\omega}'_2; \tilde{\omega}_2, \tilde{\omega}_1) \\ &+ \pi \frac{u_l}{2} [\dot{\tilde{F}}_l(\tilde{\omega}_1 - \tilde{\omega}'_2) + \dot{\tilde{F}}_l(\tilde{\omega}_2 - \tilde{\omega}'_1)], \end{aligned} \quad (3.25)$$

$$\begin{aligned} \partial_l \tilde{\Gamma}_l^{\tilde{c}c\phi\phi}(\tilde{\omega}_1, \tilde{\omega}_2; \tilde{\Omega}_1, \tilde{\Omega}_2) &= (1 - \eta_l - \gamma_l - \tilde{\omega}_1 \partial_{\tilde{\omega}_1} - \tilde{\omega}_2 \partial_{\tilde{\omega}_2} - \tilde{\Omega}_1 \partial_{\tilde{\Omega}_1} - \tilde{\Omega}_2 \partial_{\tilde{\Omega}_2}) \tilde{\Gamma}_l^{\tilde{c}c\phi\phi}(\tilde{\omega}_1, \tilde{\omega}_2; \tilde{\Omega}_1, \tilde{\Omega}_2) \\ &+ \pi \frac{u_l}{2} [\dot{\tilde{G}}_l(\tilde{\omega}_1 + \tilde{\Omega}_1) + \dot{\tilde{G}}_l(\tilde{\omega}_2 + \tilde{\Omega}_1) + \dot{\tilde{G}}_l(\tilde{\omega}_1 + \tilde{\Omega}_2) + \dot{\tilde{G}}_l(\tilde{\omega}_2 + \tilde{\Omega}_2)]. \end{aligned} \quad (3.26)$$

These linear first-order partial differential equations can be solved analytically [14]. For the external frequencies needed in Eqs. (3.19) and (3.20) we obtain

$$\tilde{\Gamma}_l^{\tilde{c}\tilde{c}cc}(\tilde{\omega}, \tilde{\omega}'; \tilde{\omega}', \tilde{\omega}) = e^{\int_0^l d\tau (1-2\eta_\tau)} \tilde{\Gamma}_0^{\tilde{c}\tilde{c}cc}(e^{-l}\tilde{\omega}, e^{-l}\tilde{\omega}'; e^{-l}\tilde{\omega}', e^{-l}\tilde{\omega}) + \pi \int_0^l dt e^{\int_{l-t}^l d\tau (1-2\eta_\tau)} u_{l-t} \dot{\tilde{F}}_{l-t}(e^{-t}(\tilde{\omega} - \tilde{\omega}')), \quad (3.27)$$

$$\begin{aligned} \tilde{\Gamma}_l^{\tilde{c}c\phi\phi}(\tilde{\omega}; \tilde{\omega}; -\tilde{\Omega}, \tilde{\Omega}) &= e^{\int_0^l d\tau (1-\eta_\tau - \gamma_\tau)} \tilde{\Gamma}_0^{\tilde{c}c\phi\phi}(e^{-l}\tilde{\omega}; e^{-l}\tilde{\omega}; -e^{-l}\tilde{\Omega}, e^{-l}\tilde{\Omega}) \\ &+ \pi \int_0^l dt e^{\int_{l-t}^l d\tau (1-\eta_\tau - \gamma_\tau)} u_{l-t} [\dot{\tilde{G}}_{l-t}(e^{-t}(\tilde{\omega} - \tilde{\Omega})) + \dot{\tilde{G}}_{l-t}(e^{-t}(\tilde{\omega} + \tilde{\Omega}))]. \end{aligned} \quad (3.28)$$

After substituting these expressions into Eqs. (3.19) and (3.20) and performing the frequency integrations we obtain

$$\begin{aligned} \dot{\Sigma}_l(\tilde{\omega}) &= \frac{1}{2} \int_0^l dt u_{l-t} \left\{ \frac{e^{\int_{l-t}^l d\tau (1-2\eta_\tau)}}{1 + r_{l-t}} \left[\frac{\delta(e^{-t}|1 - \tilde{\omega}| - 1)}{\tilde{\mu}_l + ib_l} + \frac{\delta(e^{-t}|1 + \tilde{\omega}| - 1)}{\tilde{\mu}_l - ib_l} \right] \right. \\ &\left. + \frac{e^{\int_{l-t}^l d\tau (1-\eta_\tau - \gamma_\tau)}}{1 + r_l} \left[\frac{\delta(e^{-t}|1 - \tilde{\omega}| - 1)}{\tilde{\mu}_{l-t} - ib_{l-t} \text{sgn}(1 - \tilde{\omega})} + \frac{\delta(e^{-t}|1 + \tilde{\omega}| - 1)}{\tilde{\mu}_{l-t} + ib_{l-t} \text{sgn}(1 + \tilde{\omega})} \right] \right\}, \end{aligned} \quad (3.29)$$

$$\dot{\Pi}_l(\tilde{\Omega}) = p \int_0^l dt u_{l-t} e^{\int_{l-t}^l d\tau (1-\eta_\tau - \gamma_\tau)} \text{Re} \left[\frac{\delta(e^{-t}|1 - \tilde{\Omega}| - 1)}{(\tilde{\mu}_l + ib_l)(\tilde{\mu}_{l-t} + ib_{l-t} \text{sgn}(1 - \tilde{\Omega}))} + \frac{\delta(e^{-t}|1 + \tilde{\Omega}| - 1)}{(\tilde{\mu}_l + ib_l)(\tilde{\mu}_{l-t} + ib_{l-t} \text{sgn}(1 + \tilde{\Omega}))} \right], \quad (3.30)$$

where we have introduced the shifted rescaled chemical potential,

$$\tilde{\mu}_l = \mu_l + a_l. \quad (3.31)$$

Assuming $|\tilde{\omega}| < 1$ and $|\tilde{\Omega}| < 1$ and using the fact that in this case the δ functions can be written as

$$\delta(e^{-t}|1 \pm \tilde{\omega}| - 1) = \delta(t - \ln(1 \pm \tilde{\omega})), \quad (3.32)$$

we can now carry out the t integrations. Defining $L_{\tilde{\omega}} = \ln(1 + |\tilde{\omega}|)$ and assuming $l > L_{\tilde{\omega}}$ and $l > L_{\tilde{\Omega}}$ we finally obtain

$$\dot{\Sigma}_l(\tilde{\omega}) = \frac{u_{l-L_{\tilde{\omega}}}}{2} \left[\frac{e^{\int_{l-L_{\tilde{\omega}}}^l d\tau (1-2\eta_\tau)}}{(1 + r_{l-L_{\tilde{\omega}}})(\tilde{\mu}_l - ib_l \text{sgn}\omega)} + \frac{e^{\int_{l-L_{\tilde{\omega}}}^l d\tau (1-\eta_\tau - \gamma_\tau)}}{(1 + r_l)(\tilde{\mu}_{l-L_{\tilde{\omega}}} + ib_{l-L_{\tilde{\omega}}} \text{sgn}\omega)} \right], \quad (3.33)$$

$$\dot{\Pi}_l(\tilde{\Omega}) = pu_{l-L_{\tilde{\Omega}}} e^{\int_{l-L_{\tilde{\Omega}}}^l d\tau (1-\eta_\tau - \gamma_\tau)} \text{Re} \left[\frac{1}{(\tilde{\mu}_l + ib_l)(\tilde{\mu}_{l-L_{\tilde{\Omega}}} + ib_{l-L_{\tilde{\Omega}}})} \right]. \quad (3.34)$$

The flow equations for μ_l and r_l can now be obtained from Eqs. (3.33) and (3.34) by setting the external frequencies equal to zero,

$$\begin{aligned}\partial_l \mu_l &= (1 - \eta_l) \mu_l - \dot{\Sigma}_l(0) \\ &= (1 - \eta_l) \mu_l - u_l \frac{\tilde{\mu}_l}{(1 + r_l)(b_l^2 + \tilde{\mu}_l^2)},\end{aligned}\quad (3.35)$$

$$\begin{aligned}\partial_l r_l &= (1 - \gamma_l) r_l + \dot{\Pi}_l(0) \\ &= (1 - \gamma_l) r_l - pu_l \frac{b_l^2 - \tilde{\mu}_l^2}{(b_l^2 + \tilde{\mu}_l^2)^2}.\end{aligned}\quad (3.36)$$

To determine the scale-dependent anomalous dimensions η_l and γ_l we need the linear terms in the expansions of $\dot{\Sigma}_l(\tilde{\omega})$ and $\dot{\Pi}_l(\tilde{\Omega})$,

$$\dot{\Sigma}_l(\tilde{\omega}) = \dot{\Sigma}_l(0) - \alpha_l |\tilde{\omega}| - \beta_l i \tilde{\omega} + \mathcal{O}(\tilde{\omega}^2),\quad (3.37)$$

$$\dot{\Pi}_l(\tilde{\Omega}) = \dot{\Pi}_l(0) + \gamma_l |\tilde{\Omega}| + \mathcal{O}(\tilde{\Omega}^2).\quad (3.38)$$

The fermionic anomalous dimension is then given by

$$\eta_l = a_l \alpha_l + b_l \beta_l,\quad (3.39)$$

where a_l and b_l satisfy

$$\partial_l a_l = -\eta_l a_l + \alpha_l,\quad (3.40)$$

$$\partial_l b_l = -\eta_l b_l + \beta_l,\quad (3.41)$$

with

$$\begin{aligned}\alpha_l &= \frac{u_l}{2(1 + r_l)} \left\{ \frac{\tilde{\mu}_l}{(b_l^2 + \tilde{\mu}_l^2)} \left[2 - \eta_l - \gamma_l - \frac{\partial_l r_l}{1 + r_l} \right] \right. \\ &\quad \left. + \frac{(b_l^2 - \tilde{\mu}_l^2) \partial_l \tilde{\mu}_l - \tilde{\mu}_l \partial_l b_l^2}{(b_l^2 + \tilde{\mu}_l^2)^2} \right\},\end{aligned}\quad (3.42)$$

$$\begin{aligned}\beta_l &= \frac{u_l}{2(1 + r_l)} \left\{ \frac{b_l}{(b_l^2 + \tilde{\mu}_l^2)} \left[\eta_l - \gamma_l - \frac{\partial_l r_l}{1 + r_l} \right] \right. \\ &\quad \left. + \frac{(b_l^2 - \tilde{\mu}_l^2) \partial_l b_l + b_l \partial_l \tilde{\mu}_l^2}{(b_l^2 + \tilde{\mu}_l^2)^2} \right\}.\end{aligned}\quad (3.43)$$

Finally, the bosonic anomalous dimension is

$$\gamma_l = pu_l \left[\frac{(1 - \eta_l)(b_l^2 - \tilde{\mu}_l^2)}{(b_l^2 + \tilde{\mu}_l^2)^2} + \text{Re} \frac{\partial_l(\tilde{\mu}_l + ib_l)}{(\tilde{\mu}_l + ib_l)^3} \right].\quad (3.44)$$

IV. NON-FERMI LIQUID FIXED POINT

To find possible fixed points of the above system of differential equations, we note that the flow equation (3.12) for the coupling u_l implies that at a nontrivial fixed point with $\lim_{l \rightarrow \infty} u_l = u_* \neq 0$ the fermionic and bosonic anomalous dimensions must satisfy the scaling relation

$$\gamma_* = 2 - 2\eta_*.\quad (4.1)$$

Using this to eliminate γ_* in favor of η_* we find that the fixed point values μ_* , r_* , a_* , b_* , η_* , and u_* of the six scale-dependent parameters μ_l , r_l , a_l , b_l , η_l , and u_l are constrained

by the following six equations,

$$(1 - \eta_*) \mu_* = \frac{u_*(\mu_* + a_*)}{(1 + r_*)[b_*^2 + (\mu_* + a_*)^2]},\quad (4.2a)$$

$$(2\eta_* - 1)r_* = pu_* \frac{b_*^2 - (\mu_* + a_*)^2}{[b_*^2 + (\mu_* + a_*)^2]^2},\quad (4.2b)$$

$$\eta_* a_* = \frac{\eta_* u_*(\mu_* + a_*)}{2(1 + r_*)[b_*^2 + (\mu_* + a_*)^2]},\quad (4.2c)$$

$$\eta_* b_* = \frac{(3\eta_* - 2)u_* b_*}{2(1 + r_*)[b_*^2 + (\mu_* + a_*)^2]},\quad (4.2d)$$

$$(1 - \eta_*) = (1 - \eta_*) \frac{pu_*}{2} \frac{b_*^2 - (\mu_* + a_*)^2}{[b_*^2 + (\mu_* + a_*)^2]^2},\quad (4.2e)$$

$$a_*^2 + b_*^2 = 1.\quad (4.2f)$$

We have analytically determined the solutions of this system of equations. For $u_* > 0$ we find physically acceptable solutions only for $\mu_* = a_* = 0$ implying $b_* = 1$. Actually, if we allow for (unphysical) complex values of η_* the above system has additional solutions where μ_* , a_* , and b_* are all finite. Moreover, for negative u_* we find additional solutions with $b_* = 0$, $a_* = \pm 1$, and finite μ_* , which we do not further discuss in this paper [25]. To determine the values of η_* , r_* , and u_* at the physical fixed point, we set $\mu_* = a_* = 0$ and $b_* = 1$ in Eqs. (4.2) and obtain

$$u_* = \frac{2}{p},\quad (4.3a)$$

$$r_* = \frac{2}{2\eta_* - 1},\quad (4.3b)$$

$$p\eta_* = \frac{3\eta_* - 2}{1 + r_*} = \frac{3\eta_* - 2}{1 + \frac{2}{2\eta_* - 1}}.\quad (4.3c)$$

The resulting quadratic equation for η_* has the two solutions

$$\eta_*^+ = \frac{7 + p + \sqrt{1 + 30p + p^2}}{4(3 - p)},\quad (4.4a)$$

$$\eta_*^- = \frac{4}{7 + p + \sqrt{1 + 30p + p^2}}.\quad (4.4b)$$

We discard the η_*^+ solution because it exhibits a singularity at $p = 3$ that we believe to be unphysical. The only physical solution of our fixed point equation (4.3c) for the fermionic anomalous dimension is therefore $\eta_* \equiv \eta_*^-$ given in Eq. (4.4b), which is shown in Fig. 5(a). Obviously, $\eta_*(p)$ is a continuous function of p for all p with

$$\eta_* = \frac{1}{2} - p + \mathcal{O}(p^2),\quad (4.5)$$

for small p , while for large p the leading asymptotics is

$$\eta_* = \frac{2}{p} + \mathcal{O}(1/p^2).\quad (4.6)$$

The corresponding fixed point values of r_* and u_* are shown in Fig. 5(b). Note that $1 + r_*$ is negative for all p and diverges for $p \rightarrow 0$ as $r_* \sim -1/p = -u_*/2$. For $0 < p \ll 1$ both $|r_*|$ and u_* are large compared with unity, indicating the nonperturbative nature of the non-Fermi liquid fixed point in this regime.

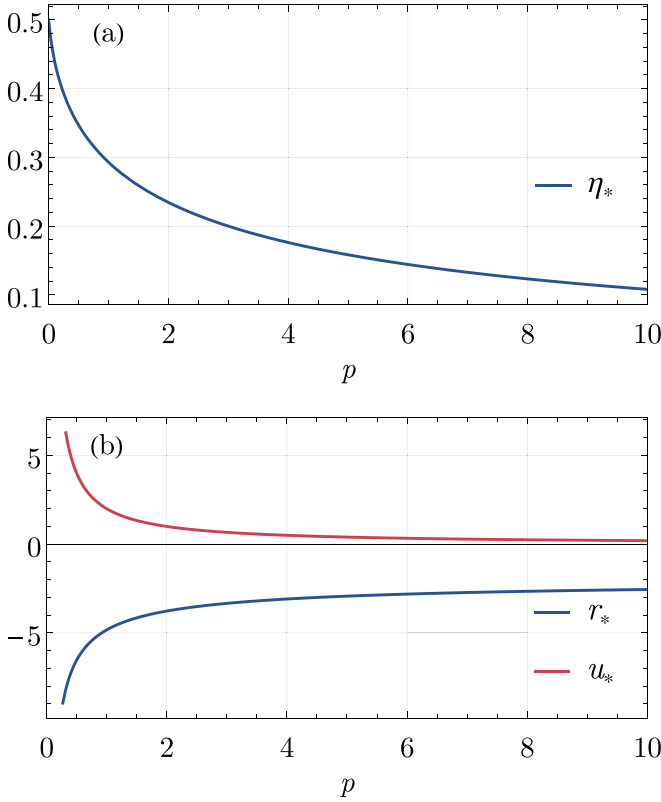


FIG. 5. (a) Physical branch $\eta_* \equiv \eta_*^-$ of the fermionic anomalous dimension at the non-Fermi liquid fixed point given in Eq. (4.4b). (b) Corresponding fixed point values of r_* (blue) and u_* (red).

Given the fact that $\gamma_* = 2 - 2\eta_* > 1$, we conclude that for small imaginary frequencies the boson propagator scales as

$$F(\Omega) \sim -k_* |\Omega|^{\gamma_* - 1}, \quad (4.7)$$

with some positive real constant k_* . For $p \rightarrow \infty$ where $\gamma_* \rightarrow 2$ this implies $F(\Omega) \sim -k_* |\Omega|$, so that the analytic continuation from the upper frequency plane to real frequencies ($|\Omega| \rightarrow -i\Omega$) gives for the retarded boson propagator

$$F_{\text{ret}}(\Omega + i0) \sim ik_* \Omega. \quad (4.8)$$

The resulting spectral function satisfies

$$\Omega \text{Im} F_{\text{ret}}(\Omega + i0) \geq 0, \quad (4.9)$$

which is a general property of any bosonic spectral function. For finite p where $1 < \gamma_* < 2$ we have to choose the physical Riemann sheet of the multi-valued complex function $z^{\gamma_* - 1}$ to obtain the physical spectral function that satisfies the positivity condition (4.9), see Ref. [26] for a careful discussion.

To investigate the stability of the non-Fermi liquid fixed point, we now study the linearized RG flow in the vicinity of this fixed point. Given the fact that at the fixed point $\mu_* = a_* = 0$ we find from Eqs. (3.35), (3.40), and (3.42) that the linearized flow in the $\mu - a$ plane decouples from the flow of the other parameters,

$$\partial_l \begin{pmatrix} \mu_l \\ a_l \end{pmatrix} = \begin{pmatrix} M_{\mu\mu} & M_{\mu a} \\ M_{a\mu} & M_{aa} \end{pmatrix} \begin{pmatrix} \mu_l \\ a_l \end{pmatrix}, \quad (4.10)$$

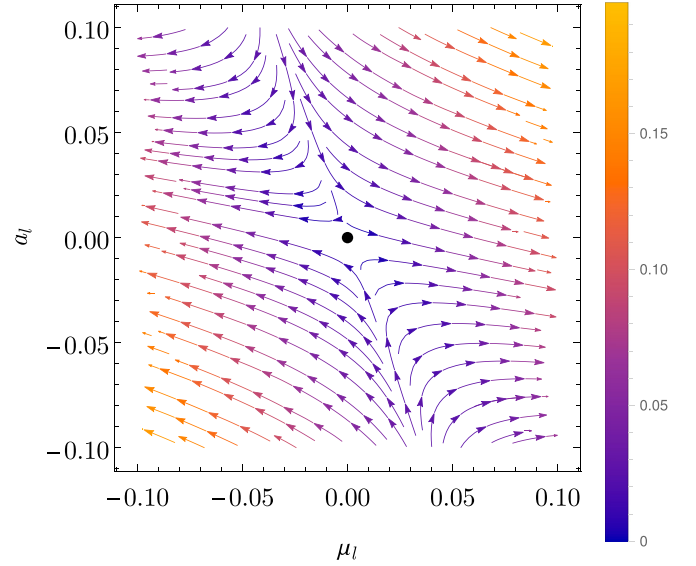


FIG. 6. RG flow in the $\mu - a$ plane for $p=1$ close to the fixed point $\mu_* = a_* = 0$ obtained from the linearized flow equations (4.10). Note that the physical initial condition corresponding to the bare action is given by the horizontal line $a_0 = 0$.

with

$$M_{\mu\mu} = 1 - \eta_* - \frac{u_*}{1 + r_*}, \quad (4.11a)$$

$$M_{\mu a} = -\frac{u_*}{1 + r_*}, \quad (4.11b)$$

$$M_{a\mu} = u_* \left(\frac{1}{1 + r_*} - \frac{1}{2(1 + r_*) - u_*} \right), \quad (4.11c)$$

$$M_{aa} = -\eta_* - \frac{u_*^2}{(1 + r_*)[2(1 + r_*) - u_*]}. \quad (4.11d)$$

The resulting RG flow in the $\mu - a$ plane is shown in Fig. 6. Obviously, the RG flow in the $\mu - a$ plane has one attractive

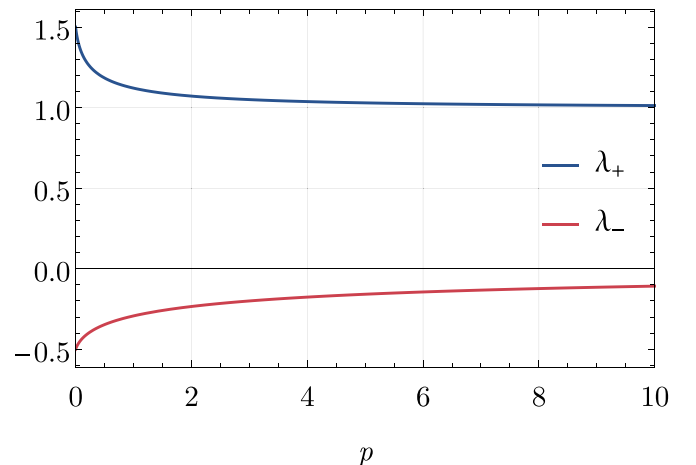


FIG. 7. Graph of the eigenvalues λ_+ (blue) and λ_- (red) of the matrix in Eq. (4.10), which characterize the linearized RG flow in the $\mu - a$ plane around the fixed point $\mu_* = a_* = 0$.

and one repulsive direction. To characterize the behavior of the RG trajectories quantitatively, we calculate the eigenvalues λ_{\pm} of the 2×2 matrix in Eq. (4.10),

$$\lambda_{\pm} = \frac{M_{\mu\mu} + M_{aa}}{2} \pm \sqrt{\left(\frac{M_{\mu\mu} - M_{aa}}{2}\right)^2 + M_{\mu a}M_{a\mu}}. \quad (4.12)$$

At small and large p , they behave as

$$\lambda_{+} = \frac{3}{2} - 3p + \mathcal{O}(p^2), \quad (4.13a)$$

$$\lambda_{-} = -\frac{1}{2} + p + \mathcal{O}(p^2), \quad (4.13b)$$

and

$$\lambda_{+} = 1 + \mathcal{O}(1/p^2), \quad (4.14a)$$

$$\lambda_{-} = -\frac{2}{p} + \mathcal{O}(1/p^2), \quad (4.14b)$$

respectively. We plot these eigenvalues as function of p in Fig. 7.

$$\lambda_r = 2\eta_* - 1 - \frac{pr_*u_*^2(5\eta_* - 3)}{2(1+r_*)^2 - (1+r_*)u_* - pu_*^2}, \quad (4.18a)$$

$$\lambda_{ru} = -p + pr_* \frac{pu_*^2 + 2(1+r_*)^2(\eta_* - 1) + u_*(1+r_*)(2\eta_* - 1)}{2(1+r_*)^2 - (1+r_*)u_* - pu_*^2}. \quad (4.18b)$$

The eigenvalue λ_r as a function of p is represented by the blue line in Fig. 8. It is always negative and has the asymptotics

$$\lambda_r = -\frac{1}{2} - 6p + \mathcal{O}(p^2), \quad (4.19a)$$

$$\lambda_r = -1 - \frac{8}{p} + \mathcal{O}(1/p^2) \quad (4.19b)$$

for small and large p , respectively. A projection of the linearized RG flow onto the plane spanned by δr_l and δu_l in the vicinity of the fixed point is shown in Fig. 9. Note that the projected flow has only attractive directions, so that fine tuning of the couplings r_l and u_l is not necessary to realize

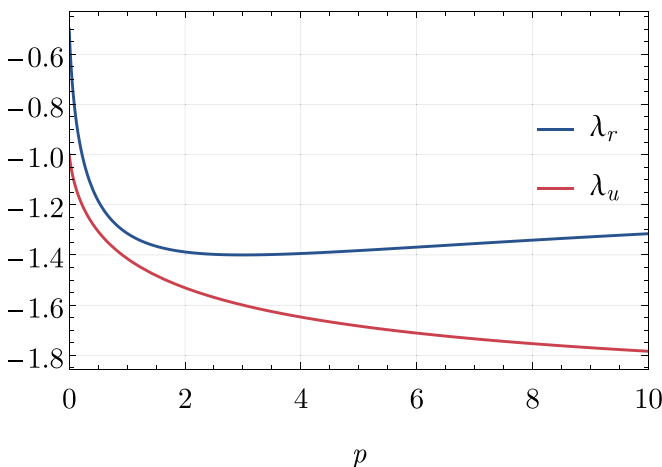


FIG. 8. Graph of the eigenvalues λ_r (blue) and λ_u (red) of the linearized flow in the vicinity of the non-Fermi liquid fixed point, see Eqs. (4.16) and (4.18a).

Next, let us discuss the linearized RG flow of the couplings u_l and r_l in the vicinity of our non-Fermi liquid fixed point. Using Eqs. (3.12), (3.43), and (3.44) we find that the linearized flow of $\delta u_l = u_l - u_*$ completely decouples from the other parameters,

$$\partial_l \delta u_l = -pu_*(1 - \eta_*)\delta u_l = \lambda_u \delta u_l, \quad (4.15)$$

with

$$\lambda_u = -pu_*(1 - \eta_*) = -2(1 - \eta_*), \quad (4.16)$$

where we have used Eq. (4.3a) to set $pu_* = 2$. Given the fact that $0 < \eta_* < 1/2$, we conclude that the coupling u_l is irrelevant at the non-Fermi liquid fixed point with scaling exponent $\lambda_u < 0$. A graph of λ_u as a function of p is shown by the red line in Fig. 8. Finally, using Eqs. (3.36), (3.43), and (3.44) we obtain for the linearized flow of $\delta r_l = r_l - r_*$,

$$\partial_l \delta r_l = \lambda_r \delta r_l + \lambda_{ru} \delta u_l, \quad (4.17)$$

where

the critical state associated with the non-Fermi liquid fixed point. Our model therefore exhibits self-tuned criticality [5] with respect to the bosonic mass parameter $\Delta + \Pi(0)$. Thus, the only relevant coupling at the non-Fermi liquid fixed point is the scaling variable associated with the positive eigenvalue λ_+ of the 2×2 matrix in Eq. (4.10), which is a linear combination of the rescaled chemical potential μ_l and the spectral asymmetry parameter a_l .

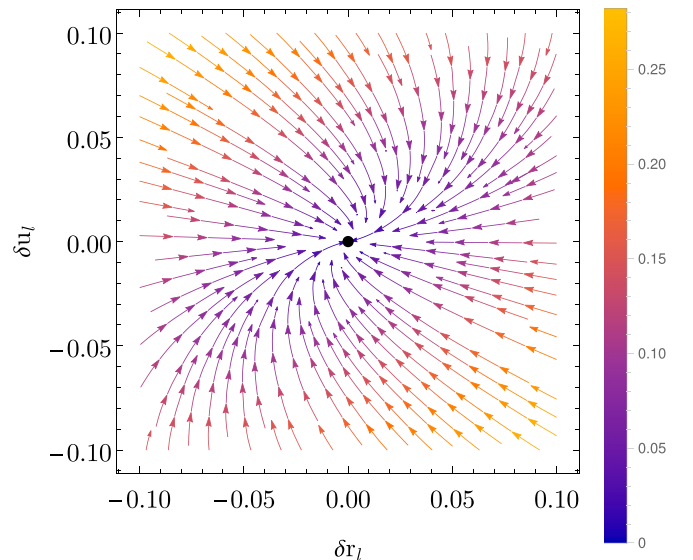


FIG. 9. RG flow in the $r - u$ plane for $p = 1$ close to the non-Fermi liquid fixed point obtained from the linearized flow equations (4.15) and (4.17).

V. SUMMARY AND CONCLUSIONS

In this paper we have developed a FRG approach for a dissipative Yukawa-SYK model where the inverse boson propagator exhibits a nonanalytic $|\Omega|$ frequency dependence. We have shown that, to leading order in $1/N$ and $1/M$, the infinite hierarchy of FRG flow equations for this model can be reduced to a system of flow equations for the irreducible fermionic and bosonic self-energies and two types of scale-dependent four-point vertices. This system is closed because the flow of the four-point vertices can be expressed again in terms of the self-energies. Within a standard low-energy expansion of the self-energies we have found a nontrivial non-Fermi liquid fixed point with critical exponents depending on the ratio N/M . A stability analysis of the linearized RG flow in the vicinity of this fixed point shows that it has only one repulsive direction corresponding to a linear combination of the rescaled chemical potential μ_l and a parameter a_l , which quantifies the spectral asymmetry. As $a_0 = 0$ in the microscopic action, the physical parameter that can be tuned to reach the non-Fermi liquid fixed point is the fermionic density. In particular, the rescaled boson mass parameter r_l and the Yukawa coupling u_l are both irrelevant at the fixed point, so that no fine-tuning of these parameters is necessary to realize the corresponding non-Fermi liquid phase. Although

in principle it should also be possible to extract these results from the corresponding Dyson-Schwinger equations, in practice our approach based on FRG flow equations is more convenient because it allows us to extract the low-energy properties analytically using well-established approximations.

It would be interesting to extend our analysis to the usual YSYK model where the inverse boson propagator exhibits a quadratic frequency dependence. Our FRG flow equations (2.48)–(2.51) remain valid also in this case, so that from a numerical solution of these equations we expect to recover the non-Fermi liquid solution of the Dyson-Schwinger equations derived in Ref. [6]. Unfortunately, the low-energy expansion of Sec. III, which is crucial to make progress analytically, does not produce sensible results in this case, at least when it is combined with a sharp frequency regulator. Possibly, an ultrasoft regulator of the type proposed by Husemann and Salmhofer [27] might solve this problem.

ACKNOWLEDGMENTS

We thank Olexandr Tsypliyatyev for useful discussions and the Deutsche Forschungsgemeinschaft (DFG, German Research Foundation) for financial support via TRR 288 - 422213477.

-
- [1] I. Esterlis and J. Schmalian, Cooper pairing of incoherent electrons: An electron-phonon version of the Sachdev-Ye-Kitaev model, *Phys. Rev. B* **100**, 115132 (2019).
 - [2] D. Hauck, M. J. Klug, I. Esterlis, and J. Schmalian, Eliashberg equations for an electron-phonon version of the Sachdev-Ye-Kitaev model: Pair-breaking in non-Fermi liquid superconductors, *Ann. Phys.* **417**, 168120 (2020).
 - [3] Y. Wang and A. V. Chubukov, Quantum phase transition in the Yukawa-SYK model, *Phys. Rev. Res.* **2**, 033084 (2020).
 - [4] Y. Wang, Solvable strong-coupling quantum-dot model with a non-Fermi liquid pairing transition, *Phys. Rev. Lett.* **124**, 017002 (2020).
 - [5] G. Pan, W. Wang, A. Davis, Y. Wang, and Z. Y. Meng, Yukawa-SYK model and self-tuned quantum criticality, *Phys. Rev. Res.* **3**, 013250 (2021).
 - [6] L. Classen and A. Chubukov, Superconductivity of incoherent electrons in the Yukawa Sachdev-Ye-Kitaev model, *Phys. Rev. B* **104**, 125120 (2021).
 - [7] A. Davis and Y. Wang, Quantum chaos and phase transition in the Yukawa-SYK model, *Phys. Rev. B* **107**, 205122 (2023).
 - [8] D. Valentinis, G. A. Inkof, and J. Schmalian, Correlation between phase stiffness and condensation energy across the non-Fermi to Fermi-liquid crossover in the Yukawa-Sachdev-Ye-Kitaev model on a lattice, *Phys. Rev. Res.* **5**, 043007 (2023).
 - [9] D. Valentinis, G. A. Inkof, and J. Schmalian, BCS to incoherent superconductivity crossovers in the Yukawa-SYK model on a lattice, *Phys. Rev. B* **108**, L140501 (2023).
 - [10] J. Kim, X. Cao, and E. Altman, Low-rank Sachdev-Ye-Kitaev models, *Phys. Rev. B* **101**, 125112 (2020).
 - [11] S. Sachdev, Bekenstein-Hawking entropy and strange metals, *Phys. Rev. X* **5**, 041025 (2015).
 - [12] A. Kitaev and S. J. Suh, The soft mode in the Sachdev-Ye-Kitaev model and its gravity dual, *J. High Energy Phys.* **05** (2018) 183.
 - [13] N. Goldenfeld, *Lectures on Phase Transitions and the Renormalization Group* (Addison-Wesley Publishing, Reading, MA, 1992).
 - [14] P. Kopietz, L. Bartosch, and F. Schütz, *Introduction to the Functional Renormalization Group* (Springer, Berlin, 2010).
 - [15] R. Smit, D. Valentinis, J. Schmalian, and P. Kopietz, Quantum discontinuity fixed point and renormalization group flow of the Sachdev-Ye-Kitaev model, *Phys. Rev. Res.* **3**, 033089 (2021).
 - [16] F. Schütz, L. Bartosch, and P. Kopietz, Collective fields in the functional renormalization group for fermions, Ward identities, and the exact solution of the Tomonaga-Luttinger model, *Phys. Rev. B* **72**, 035107 (2005).
 - [17] A. A. Katanin, Fulfillment of Ward identities in the functional renormalization group approach, *Phys. Rev. B* **70**, 115109 (2004).
 - [18] I. Aref'eva, M. Khramatsov, M. Tikhanovskaya, and I. Volovich, On replica-nondiagonal large N saddles in the SYK model, *EPJ Web Conf.* **191**, 06007 (2018).
 - [19] C. Wetterich, Exact evolution equation for the effective potential, *Phys. Lett. B* **301**, 90 (1993).
 - [20] J. Berges, N. Tetradis, and C. Wetterich, Non-perturbative renormalization flow in quantum field theory and statistical physics, *Phys. Rep.* **363**, 223 (2002).
 - [21] W. Metzner, M. Salmhofer, C. Honerkamp, V. Meden, and K. Schönhammer, Functional renormalization group approach to correlated fermion systems, *Rev. Mod. Phys.* **84**, 299 (2012).
 - [22] N. Dupuis, L. Canet, A. Eichhorn, W. Metzner, J. M. Pawłowski, M. Tissier, and N. Wschebor, The nonperturbative

functional renormalization group and its applications, [Phys. Rep. **910**, 1 \(2021\)](#).

- [23] R. Smit, Breakdown and absence of quasiparticles in Kitaev's models, Ph.D. thesis, Goethe-Universität Frankfurt, 2022.
- [24] In order to derive the single-scale propagator (3.5b) from the regularized propagator (3.5a), we have used the identity

$$\delta(x)f(\Theta(x)) = \delta(x) \int_0^1 dt f(t);$$

see T. R. Morris, The exact renormalization group and approximate solutions, [Int. J. Mod. Phys. A **09**, 2411 \(1994\)](#).

- [25] From our definition of u_l in Eq. (3.11) it is obvious that $u_l < 0$ describes a purely imaginary bare coupling g , corresponding to a purely imaginary Yukawa coupling g_{ijk} in our original

YSYK action given in Eq. (1.1). Such an imaginary Yukawa coupling generates a *repulsive* two-body interaction between the fermions when the boson field is integrated out. In contrast, a positive value of u_* is associated with an underlying attractive two-body interaction between the fermions, so that in this case the prefactor in the Dyson-Schwinger equation (2.60) for the fermionic self-energy is positive. It is therefore not surprising that for positive g^2 the YSYK model exhibits a pairing instability [6].

- [26] K. Schönhammer, Confined coherence and analytic properties of Green's functions, [Phys. Rev. B **58**, 3494 \(1998\)](#).
- [27] C. Husemann and M. Salmhofer, Efficient parametrization of the vertex function, Ω scheme, and the tt' Hubbard model at van Hove filling, [Phys. Rev. B **79**, 195125 \(2009\)](#).